Quaternary Science Reviews 55 (2012) 59–74

Contents lists available at SciVerse ScienceDirect

Quaternary Science Reviews

journal homepage: www.elsevier.com/locate/quascirev

Molecular records of climate variability and vegetation response since the Late Pleistocene in the Lake Victoria basin, East Africa

Melissa A. Berke [a,b,*], Thomas C. Johnson [a,b], Josef P. Werne [a,c,d], Kliti Grice [e], Stefan Schouten [f], Jaap S. Sinninghe Damsté [f]

[a] Large Lakes Observatory, University of Minnesota Duluth, Duluth, MN 55812, USA
[b] Department of Geological Sciences, University of Minnesota Duluth, Duluth, MN 55812, USA
[c] Department of Chemistry & Biochemistry, University of Minnesota Duluth, Duluth, MN 55812, USA
[d] Centre for Water Research, University of Western Australia, Crawley, Western Australia and WA – Organic and Isotope Geochemistry Centre, Curtin University of Technology, Bentley, WA, Australia
[e] WA-Organic and Isotopic Geochemistry Centre, Department of Chemistry, Curtin University, Perth, Australia
[f] NIOZ Royal Netherlands Institute for Sea Research, Department of Marine Organic Biogeochemistry, P.O. Box 59, Den Burg 1790 AB, Netherlands

ARTICLE INFO

Article history:
Received 24 April 2012
Received in revised form
17 August 2012
Accepted 20 August 2012
Available online

Keywords:
Africa
Tropical paleoclimate
Compound specific hydrogen and carbon isotopes
TEX_{86} temperatures
Insolation forcing
ENSO
Monsoonal precipitation

ABSTRACT

New molecular proxies of temperature and hydrology are helping to constrain tropical climate change and elucidate possible forcing mechanisms during the Holocene. Here, we examine a ~14,000 year record of climate variability from Lake Victoria, East Africa, the world's second largest freshwater lake by surface area. We determined variations in local hydroclimate using compound specific δD of terrestrial leaf waxes, and compared these results to a new record of temperature utilizing the TEX_{86} paleotemperature proxy, based on aquatic Thaumarchaeotal membrane lipids. In order to assess the impact of changing climate on the terrestrial environment, we generated a record of compound specific $\delta^{13}C$ from terrestrial leaf waxes, a proxy for ecosystem-level C_3/C_4 plant abundances, and compared the results to previously published pollen-inferred regional vegetation shifts. We observe a general coherence between temperature and rainfall, with a warm, wet interval peaking ~10–9 ka and subsequent gradual cooling and drying over the remainder of the Holocene. These results, particularly those of rainfall, are in general agreement with other tropical African climate records, indicating a somewhat consistent view of climate over a wide region of tropical East Africa. The $\delta^{13}C$ record from Lake Victoria leaf waxes does not appear to reflect changes in regional climate or vegetation. However, palynological analyses document an abrupt shift from a Poaceae (grasses)-dominated ecosystem during the cooler, arid late Pleistocene to a Moraceae-dominated (trees/shrubs) landscape during the warm, wet early Holocene. We theorize that these proxies are reflecting vegetation in different locations around Lake Victoria. Our results suggest a predominantly insolation-forced climate, with warm, wet conditions peaking at the maximum interhemispheric seasonal insolation contrast, likely intensifying monsoonal precipitation, while maximum aridity coincides with the rainy season insolation and the interhemispheric contrast gradient minima. We interpret a shift in conditions at the Younger Dryas to indicate a limited switch in insolation-dominated control on climate of the Lake Victoria region, to remote teleconnections with the coupled Atlantic and Pacific climate system.

1. Introduction

Geological evidence of extensive drought and dramatic changes in water level has been widely documented at Lake Victoria and the surrounding region in the Late Pleistocene. Seismic reflection profiles, sediment lithology, and fossil assemblages of diatoms and pollen have revealed multiple intervals of aridity, including the complete desiccation of Lake Victoria prior to 15 ka, with profound impacts on the regional fauna (Johnson et al., 1996) and flora (Stager and Mayewski, 1997; Beuning, 1999). While these studies have increased our understanding of the environmental response to aridity and the potential global climate implications captured by these records, the changes in regional climate can only be inferred

* Corresponding author. Current address: Global Change and Sustainability Center, University of Utah, Salt Lake City, UT 84112, USA.
E-mail address: melissa.berke@utah.edu (M.A. Berke).

0277-3791/$ – see front matter © 2012 Elsevier Ltd. All rights reserved.
http://dx.doi.org/10.1016/j.quascirev.2012.08.014

in a qualitative sense. The advent and usage of novel molecular techniques and compound specific isotope analyses have provided additional proxies to document and quantify changes in tropical moisture balance and thermal excursions, highlighting not only the effects of reconstructed climate change, but also the regional drivers. It is often cited that tropical ecosystems are more sensitive to perturbations in hydrology than temperature (Schefuß et al., 2003; Castañeda et al., 2007), due to the limited thermal range of tropical climate. But with a paucity of continental temperature reconstructions, the full range of tropical temperatures through time is unknown. Ultimately, the new molecular proxy reconstructions (e.g. Powers et al., 2005; Tierney et al., 2008, 2010; Konecky et al., 2011) allow for an independent measure of the hydrologic and temperature shifts occurring in an area, and thus may elucidate what regional and extratropical forcing is relevant to the climate of equatorial East Africa.

To constrain the hydrologic and temperature variability associated with climate change in the Lake Victoria basin, we investigate the regional rainout history using compound specific δD on the dominant terrestrial leaf waxes and a record of paleotemperature reconstructed using the TEX_{86} proxy from a Lake Victoria sediment core. TEX_{86} and δD are used to determine the degree to which moisture and temperature are connected over millennial time scales in this portion of the equatorial tropics. Modeling studies suggest coupled hydrologic response with temperature (Jolly et al., 1998), and we aim to determine if the relationship between precipitation and temperature is consistent over longer time scales. We then consider the influence of precipitation and temperature variability on regional vegetation by comparing a new record of $\delta^{13}C$ in leaf waxes from terrestrial higher plants in the same sediment samples to pollen reconstructions from Lake Victoria by Kendall (1969). These molecular proxies have been successfully applied elsewhere in tropical East and West Africa (e.g. Powers et al., 2005; Weijers et al., 2007; Tierney et al., 2008; Niedermeyer et al., 2010; Konecky et al., 2011; Sinninghe Damsté et al., 2011) over the Late Pleistocene and Holocene and thus allow for comparison within a larger regional context. These proxies will be discussed further in Sections 2.2 and 2.3.

2. Background

2.1. Lake Victoria regional setting

Lake Victoria is the largest lake by surface area in Africa, covering ~69,000 km^2. It is fairly shallow, with a mean water depth of ~40 m, and a maximum water depth of ~79 m (Crul, 1995). Despite the lake's large surface area, the catchment is rather small, extending less than three times larger than the lake itself, ~190,000 km^2 (Yin and Nicholson, 1998). Lake Victoria is an open basin, with the largest inflowing river, the Kagera, entering via the western shore (Fig. 1). The lake serves as the headwaters to the Nile River, with the White Nile (or Victoria Nile), exiting in the north and traveling through Lake Albert and across the Sudan, before connecting with the Blue Nile to form the Nile River. The majority of water to the lake is derived from direct precipitation (>80%), with ~70% of water loss from the basin being attributed to evaporation (Beadle, 1981; Yin and Nicholson, 1998).

While Lake Victoria experiences many smaller mixing events, it is monomictic, with one annual overturn of the entire water column occurring between May and August due to a seasonal increase of regional trade winds. Measurements taken in 1952–1954 show that annual water temperatures range from 24 to 26.6 °C, and surface waters exhibit ≤2 °C difference with bottom waters at any time during the year (Fish, 1957; Talling, 1957). The region receives annual precipitation totaling ~1200–1600 mm/yr (Nicholson, 1988; Sene and Plinston, 1994), peaking in March–April–May (MAM; known as the long rains) and November–December (known as the short rains) (Nicholson, 1996). The delivery is governed in large part by the twice annual meridional migration of the Intertropical Convergence Zone (ITCZ), a zone of low pressure where the Northern and Southern Hemisphere trade winds meet, whose mean position moves seasonally due to interhemispheric temperature gradients (Nicholson, 1996). Additionally, the area is influenced by the Congo Air Boundary (CAB), a humid, unstable air confluence with seasonal zonal movement, marking the intersection of air masses containing moisture derived from the West African Congo Basin (derived from the Atlantic Ocean) and the western Indian Ocean (Nicholson, 1996). The modern ITCZ and CAB are located well to the north of Lake Victoria beginning in August and to the south of the basin in January, generally producing two distinct wet seasons, with easterly and southeasterly winds generally supplying moisture to the region (Levin et al., 2009).

2.2. The TEX_{86} temperature proxy

A number of African lake temperature records have been produced through the application of the TEX_{86} temperature proxy. TEX_{86} is based on the number of cyclopentane moieties of isoprenoid glycerol dialkyl glycerol tetraethers (GDGTs), membrane lipids from aquatic Thaumarchaeota, previously referred to as Crenarchaeota (Brochier-Armanet et al., 2008), which are well preserved in marine and lacustrine sediments (Schouten et al., 2002; Kim et al., 2010; Powers et al., 2010). The distribution of these GDGTs correlates with surface water temperature in the oceans and some lakes, and thereby provides the opportunity to reconstruct past temperature (Schouten et al., 2002; Blaga et al., 2009; Kim et al., 2010; Powers et al., 2010). Studies have shown that temperature primarily influences the TEX_{86} proxy, suggesting it is independent of changes in salinity, nutrients, or hydrology (Schouten et al., 2002; Wuchter et al., 2004; Kim et al., 2010), though there is still much that is unknown about the ecology and thus habitat of the TEX_{86}-generating Thaumarchaeota.

In some lakes, substantial amounts of soil-derived isoprenoid tetraether compounds confound the signal derived from aquatic Thaumarchaeota (Blaga et al., 2009; Powers et al., 2010) and thus TEX_{86} may not be a reliable proxy for past temperature. This terrestrial influence is quantified by the BIT (Branched and Isoprenoid Tetraether) index, a ratio of branched GDGTs (predominantly soil-derived) to crenarchaeol, an isoprenoid GDGT that has so far only been detected in Thaumarchaeota. The BIT index ranges from <0.1 (predominantly aquatic) to >0.9 (predominantly terrestrial) (Hopmans et al., 2004). TEX_{86} is not considered to be a reliable recorder of past temperature in lake sediment when BIT values exceed ~0.4 (Blaga et al., 2009).

2.3. $\delta^{13}C$ and δD of leaf wax compounds

The $\delta^{13}C$ and δD of compounds derived mainly from fossil epicuticular leaf waxes, such as long chain odd-carbon numbered *n*-alkanes or even-carbon numbered *n*-alkanoic acids (Eglinton and Hamilton, 1967), are frequently used to reconstruct changing higher plant communities and precipitation (Collister et al., 1994; Sachse et al., 2004; Chikaraishi and Naraoka, 2007; Hou et al., 2008). Epicuticular waxes are easily abraded from leaf surfaces by wind or rain and can be transported via aeolian or fluvial pathways, and are generally well preserved in sediments (Huang et al., 2000; Schefuß et al., 2003). Consequently, lacustrine sediments contain a mixture of leaf waxes derived from regional and more proximal

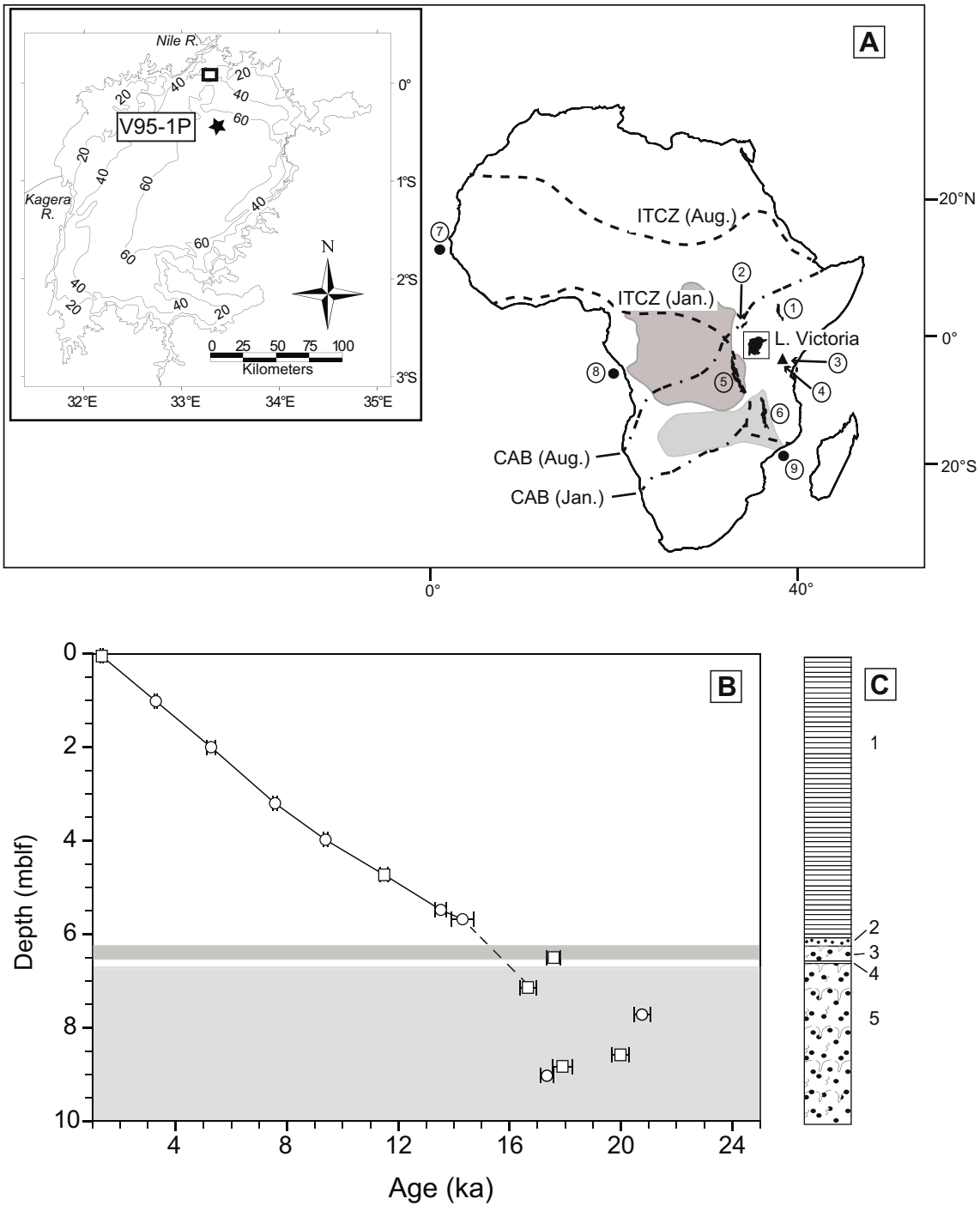

Fig. 1. (A) Map of Africa, showing locations of East and West African sites described in text: 1) Lake Turkana, 2) Lake Albert, 3) Mt. Kilimanjaro, 4) Lake Challa, 5) Lake Tanganyika, 6) Lake Malawi, 7) Senegal River drainage (West Sahel), GeoB9508-5, 8) Congo Basin, GeoB 6518-1, 9) Zambezi River catchment, GeoB9307-3. Generalized ITCZ/CAB air boundary locations (dashed lines) are shown (Nicholson, 1996; Leroux, 2001). Position of Lake Victoria: sediment core V95-1P (this study) denoted with a star and core 64–4 pollen (open square) (Kendall, 1969) are also shown; (B) Age model for V95-1P, based on new radiocarbon dates, denoted with squares (Table 1), and a published chronology (Johnson et al., 2000), denoted with circles, and associated error bars. The age model is based on linear interpolation between calibrated radiocarbon dates above 568 cm depth (14,315 ka), and is extrapolated to the youngest date into the paleosol below, represented by the dashed line. Paleosols are indicated by shaded areas; (C) Generalized sediment description based on Talbot and Lærdal (2000) as follows: 1) uniform very fine grained mud and abundant diatoms; 2) transitional sediments, few to no diatoms, crumbly texture; 3) no diatoms, crumbly texture, sandy, vertically cracked with rootlets present; 4) transitional silty/sandy mud, abundant sponge spicules; 5) return to no diatoms, crumbly texture, sandy, vertically cracked with rootlets.

vegetation whose *n*-alkane chain length and isotopic signature can be used to distinguish vegetation types (Cranwell et al., 1987; Collister et al., 1994).

There are two primary CO_2 fixation pathways used by terrestrial plants that have distinct isotopic signals, allowing the use of $\delta^{13}C$ to distinguish regional vegetation change (O'Leary, 1981). The C_3 (Calvin–Benson) and C_4 (Hatch–Slack) metabolic pathways have differing enzymatic processes that govern how atmospheric CO_2 is utilized and thus what isotopic signal is imparted to the plants (O'Leary, 1981). C_3 plants, predominantly

shrubs and trees, use ribulose bisphosphate carboxylase–oxygenase (Rubisco) for initial carboxylation, and have high rates of photorespiration (O'Leary, 1981; Tipple and Pagani, 2007). C_4 plants, predominantly grasses and sedges, have more efficient utilization of CO_2 via a pre-concentrating mechanism that utilizes the enzyme phosphoenolpyruvate-carboxylase (PEP-C) and concentrates CO_2 at the active site of Rubisco, reducing photorespiration and consequently the carbon isotope fractionation observed (Hatch, 1987; Taiz and Zeiger, 1998; Tipple and Pagani, 2007). The carbon concentrating mechanism employed by C_4 plants allows them to have an ecological advantage in warmer, drier, or low pCO_2 environments (Cerling et al., 1997; Ehleringer et al., 1997) due to their ability to curb possible desiccation by closing stomata and reducing transpiration and CO_2 loss. The end result of these different photosynthetic pathways is that C_3 plants have a characteristically ^{13}C-depleted carbon isotope signature compared to C_4 plants (Rieley et al., 1993; Collister et al., 1994; Castañeda et al., 2009b). A third photosynthetic pathway, CAM (Crassulacean Acid Metabolism), found in succulents and involving CO_2 uptake and fixation at night, is not thought to be a significant component of the vegetation in this region (White, 1983). Furthermore, while atmospheric $\delta^{13}C$ has changed through the interval described in this study (Indermuhle et al., 1999), the changes have been minor (0.3‰ shift during the Holocene), and are within the mean replicate error of samples measured from Lake Victoria.

The δD of plant compounds tracks the δD of source water, with a biosynthetic fractionation (Sachse et al., 2004; Hou et al., 2008; Zhang et al., 2009; Polissar and Freeman, 2010; Zhou et al., 2011; Sachse et al., 2012). It has been demonstrated from isotopic investigation of water isotopes in the tropics that the $\delta^{18}O$ and δD of rainfall is inversely correlated with the amount of precipitation in the tropics (Dansgaard, 1964; Rozanski et al., 1993), and thus in times of higher rainout there is a more D-depleted signal than in times of increased aridity. This relationship assumes that other factors that could potentially influence δD of leaf waxes remain constant or can be constrained by other proxy data. Recent studies have demonstrated the utility of δD in determining hydroclimate variability in Africa (Schefuß et al., 2005; Tierney et al., 2008; Niedermeyer et al., 2010; Tierney et al., 2011) and elsewhere (Yang and Huang, 2003; Makou et al., 2007; Liu et al., 2008; Li et al., 2011).

In order to use δD as an independent aridity proxy, we must constrain changes in vegetation occurring over this interval and potential secondary effects to the δD of leaf waxes. Apparent fractionation varies widely among C_3 plants (Hou et al., 2007, 2008), yet ecosystem-wide transect studies of plant wax δD show a remarkably linear correlation with the isotopic composition of regional rainfall, across vegetation landscapes of varied species and C_3/C_4 photosynthetic pathway (Sachse et al., 2004; Hou et al., 2008; Feakins and Sessions, 2010; Sachse et al., 2012). The consistency may imply that a regional integration of the isotopic fractionation is being preserved in the sediments and might mean differences in vegetation play a smaller role in δD at a broad spatial scale. Therefore, we assume that changes in precipitation played the largest role in shaping the δD signal in this record.

3. Materials and methods

3.1. Core sampling

Core V95-1P was collected in 1995 from the north central portion of the lake (01°13.9′S, 33°11.9′E) in 68 m water depth as part of the International Decade of East African Lakes (IDEAL) program. A total of 7 piston cores were recovered using a Kullenberg corer on this expedition, and we selected V95-1P for this study due to its robust age model, discussed below (Johnson et al., 2000). The sediments were in excellent condition and the entire length of piston core V95-1P was sampled (Fig. 1). There is an average sampling resolution ~250 years for the record of temperature history, and somewhat lower resolution for compound specific isotopes due to analytical time constraints.

3.2. Core sedimentology and chronology

Core V95-1P consists of a crumbly-textured mud that, beginning at ~624 cm depth, grades into a more uniform, fine-grained mud with abundant aquatic diatoms in the upper 600 cm of the core (Talbot and Lærdal, 2000) (Fig. 1). The crumbly-textured mud is interpreted as a paleosol and shows indications of subaerial exposure (vertical cracks, rootlets) and few to no aquatic fossils. A second paleosol underlies this unit, separated by a thin horizon of silty mud with macrofossils that indicates a brief transgression between major desiccation events in the Lake Victoria basin in the Late Pleistocene (Johnson et al., 1996, 2000). The age model for the core was previously published in Johnson et al. (2000) based on radiocarbon dates on the 20–70 μm fraction of pollen–lignin–charcoal, and is here supplemented by the addition of new dates on bulk organic carbon and a wood fragment (Table 1 and Fig. 1). All ages are calibrated using CalPal (Weninger et al., 2011) and are reported in calibrated ka before present (ka). The uppermost sediments in the lake were not recovered due to over-penetration by the Kullenberg corer, and the age of the sediments in the core top is estimated to be 1000 years. Radiocarbon dates increase consistently with depth to 650 cm. Dates inconsistent with burial depth are associated with paleosols, which begin below ~624 cm, perhaps due to the addition of reworked older carbon or the growth of younger plant roots into older soil. The age model is based on linear interpolation between calibrated radiocarbon dates above 568 cm depth (14.3 ka), and is extrapolated to the youngest date into the paleosol below, represented by the dashed line in Fig. 1.

3.3. Lipid extraction and separation

Freeze-dried, homogenized sediments (typically 1–3 g dry weight) were extracted using soxhlet extraction with 2:1 dichloromethane:methanol (DCM:MeOH) for 24 h to produce a total lipid

Table 1
Summary of new ^{14}C ages from core V95-1P. Calibrated to calendar years using CalPal (Weninger et al., 2011).

Core	Section	Core depth (cm)	Absolute depth (cm below lake floor)	NOSAMS #	^{14}C age	Calendar years	Material
LV95-1P	II	6.0–9	101.5	OS-77334	3060 ± 35	3288 ± 47	Sediment organic carbon
LV95-1P	V	77–81	473	OS-77335	10,000 ± 40	11,496 ± 142	Sediment organic carbon
LV95-1P	VIIa	55–58	650	OS-77351	14,450 ± 65	17,588 ± 250	Sediment organic carbon
LV95-1P	VIIb	22–24	714	OS-77314	13,600 ± 55	16,662 ± 291	Plant/wood fragment
LV95-1P	XII	24.5–26	772	OS-77350	17,300 ± 75	20,764 ± 289	Bulk organic carbon
LV95-1P	XIII	35–37	883	OS-77336	14,600 ± 60	17,901 ± 357	Bulk organic carbon

extract (TLE). All extractions were accompanied by an extraction blank that was taken through the entire procedure and tested for the presence of contaminants at each stage prior to analysis of samples. The TLE was then separated into neutral, free fatty acid, and phospholipid fatty acid fractions using an aminopropylsilyl bond elute column, cleaned prior to use with 10 mL successive rinses of MeOH followed by 1:1 DCM:2-propanol. Eight mL each of 1:1 DCM:2-propanol, 4% glacial acetic acid in distilled ethyl ether, and MeOH, were used with the cleaned columns to elute the neutral, free fatty acid, and phospholipid fatty acid fractions, respectively. Short column chromatography with activated alumina as the stationary phase was used to further separate the neutral fraction into apolar and polar fractions using 9:1 hexane:DCM followed by 1:1 DCM:MeOH as eluents for the two fractions, respectively. The polar fraction contains the GDGT lipids required for TEX_{86} analysis. The polar fraction was filtered (0.45 μm filter), dried under N_2, and then redissolved in 99:1 hexane:isopropanol for analysis. The apolar fraction containing *n*-alkanes was further separated into saturated and unsaturated hydrocarbons using Ag^+ impregnated silica gel column chromatography as described in Castañeda et al. (2007). The *n*-alkanoic (fatty acid) fractions were methylated using 5% BF_3 in methanol (100 °C for 2 h) to produce fatty acid methyl esters (FAME) (Wakeham and Pease, 1992). The resulting FAME fraction was then extracted using hexane and a NaCl solution, with residual water removed using sodium sulfate columns. FAMEs were further cleaned via extracted Si gel eluted with successive runs of DCM followed by hexane.

3.4. TEX_{86} temperature analyses and paleotemperature estimation

GDGTs were analyzed by high performance liquid chromatography/atmospheric pressure chemical ionization mass spectrometry (HPLC/MS) as described in Schouten et al. (2007). Briefly, GDGTs were analyzed using an Agilent 1100 series LC–MSD SL (Alltech Prevail Cyano column 150 × 2.1 mm; 3 μm) maintained at 30 °C for separation. Runs began with isocratic elution for 5 min, with a flow rate of 0.2 ml/min, followed by a linear gradient to 1.8% isopropanol in 45 min. Detection was achieved using atmospheric pressure positive ion chemical ionization mass spectrometry (APCI-MS) of the eluent.

Analytical error for the TEX_{86} proxy has been shown to be relatively small, on par with analytical reproducibility of other temperature proxies (Schouten et al., 2007). Reproducibility for this study was determined using replicates from a series of East African Rift Lakes ($n = 51$ from Lakes Malawi, Turkana, Albert, and Victoria) run and integrated by the same operator on the same HPLC/MS system to minimize potential variability. The mean error of all duplicates provides a TEX_{86} value of 0.007, representing an average uncertainty in temperature of ±0.3 °C using the calibration of Kim et al. (2010) as discussed below. Therefore, a standard analytical error of ±0.3 °C is plotted for all Lake Victoria TEX_{86} values.

The relationship between mean annual lake surface temperatures (LST) and TEX_{86} values are calibrated using the equation for marine sediments, TEX_{86}^{H} (Kim et al., 2010) with a temperature calibration error estimation of ~2.5 °C based on 255 global surface sediment samples. Lake Victoria surface sediment samples plot anomalously warm in the global lake calibration plot (Powers et al., 2010), but yield LST similar to those of present day when using the global marine calibration line (Kim et al., 2010). We speculate that a calibration offset for Lake Victoria may be due to a lack of a permanent chemocline and anoxic deep water, similar to that of Lake Turkana, which also shows surface sediments that plot on the warm side of the global lake calibration curve and fit the marine TEX_{86} calibration curve (Berke et al., 2012). Thaumarchaeota are known to be ammonia oxidizers (Konneke et al., 2005; Wuchter et al., 2006) and therefore may be nourished by the proximity of an oxic and anoxic water boundary where turbulent mixing can provide an ample supply of ammonia across the chemocline (Konneke et al., 2005; Coolen et al., 2007; Blaga et al., 2011). In the absence of such conditions, such as in the oceans and in Lake Victoria, a different community of Thaumarchaea may dominate and generate GDGTs that more closely tracks the marine TEX_{86} calibration curve.

3.5. *N*-alkane identification, quantification, and $\delta^{13}C$ analysis

N-alkanes were identified using an Agilent 6890 gas chromatograph (GC) coupled to an Agilent 5973 mass spectrometer (MS). An HP-1 capillary column (25 m × 32 mm × 0.5 μm) was used with He flow rates set at 2 ml/min. Quantification of *n*-alkanes was carried out using an Agilent 6890 GC with flame ionization detection (FID) using 5α-androstane as an internal standard in all samples, with GC–MS and GC–FID programs described by Castañeda et al. (2009a).

An Agilent 6890N GC (60 m HP-1 column, 0.32-um diameter, 0.25 μm film thickness) interfaced to Thermo Finnigan Delta^{Plus} XP mass spectrometer was used to determine $\delta^{13}C$ of *n*-alkanes. The GC temperature program began at 50 °C and increased at a rate of 50 °C/min to 180 °C and next at a rate of 3 °C/min to 320 °C. The final temperature of 320 °C was held for 6 min. The *n*-alkanes separated by the GC column were oxidized at 940 °C and converted to CO_2. A standard mixture of *n*-alkanes of known $\delta^{13}C$ values was analyzed multiple times daily ("Mix-A", C_{16}–C_{30} provided by Dr. Arndt Schimmelmann, Indiana University), and based on these replicate measurements, typical precision of the $\delta^{13}C$ measurements were ±0.5‰ (1σ). Each sample was run at least in duplicate, co-injected with squalane as an internal standard to monitor reproducibility of measurements, found to be better than ±0.5‰. Replicates were analyzed and are plotted individually for each *n*-alkane sample, with a mean error of ±0.3‰ for C_{29} duplicates. All $\delta^{13}C$ values are reported as per mil deviations from Vienna Pee Dee Belemnite (VPDB) standard using conventional delta notation.

3.6. δD analysis

N-alkanes are in fairly low abundance in Lake Victoria samples, which prohibited the analysis of both $\delta^{13}C$ and δD, thus another class of leaf wax compounds, *n*-alkanoic acids, was used for δD analysis. While more abundant than *n*-alkanes, limited abundances of *n*-alkanoic acids in these sediments precluded the additional analysis of $\delta^{13}C$ on this compound following δD analysis. Simultaneous methylation of fatty acid fractions with a palmitic acid standard of known value (a non-methylated palmitic acid standard was independently measured at the University of South Florida) was carried out in order to determine the isotopic composition of the attached methyl group, which was corrected for using a mass balance calculation. δD was also corrected for changes in ice volume and subsequent shifts in the δD of sea water in a manner previously described (Konecky et al., 2011; Tierney et al., 2011), assuming the LGM ocean was 1‰ more ^{18}O-enriched than present (Schrag et al., 1996) and adjusting shifts through time to the ice volume changes shown in the LR04 benthic oxygen isotope stack (Lisiecki and Raymo, 2005).

FAMEs were identified using GC/MS and quantified using GC–FID as described above for *n*-alkanes. δD of FAMEs was determined using a MicroMass IsoPrime GC–IRMS with instrumental conditions outlined in Grice et al. (2008). H_2 gas of known isotopic value and high purity grade was injected as a reference gas standard and H^{3+} correction factor was monitored daily. A mixture of 6 FAMEs of known isotopic composition was run between samples to monitor instrument accuracy. Analyses of *n*-alkanes were

performed in duplicate or triplicate, with a mean error for all samples of ±4‰. All values reported here are averages of these measurements. C_{28} was the most abundant FAME homolog measured at Lake Victoria and is hereafter referred to as δD. This study will focus on the isotopic composition of just the most abundant homolog, an approach taken previously (Schefuß et al., 2005; Tierney et al., 2008; Konecky et al., 2011; Tierney et al., 2011) due to the lack of consistently measured C_{26} (the second most abundant homolog) or C_{30} (the third most abundant) downcore. All δD values are reported as per mil deviations from Vienna Standard Mean Ocean Water (VSMOW) in conventional delta notation.

4. Results

4.1. The TEX_{86} paleotemperatures

The TEX_{86} values of core V95-1P exhibit significant variations, ranging from ~0.50–0.80 (Fig. 2). We note what appears to be the largest variability of the record in the paleosols that formed during the Late Pleistocene. The BIT index (Hopmans et al., 2004), with values ranging from ~0.9 to 0.4 below 600 cm (Fig. 2), indicates a significant contribution of soil lipids, and therefore TEX_{86} in this interval is an unreliable indicator of past lake temperatures (Weijers et al., 2006; Blaga et al., 2009; Powers et al., 2010). Previously described paleosols and suspect chronology prior to 15.2 ka (Johnson et al., 1996, 2000) coincide with this interval of terrestrially-influenced lipids and TEX_{86} temperatures (Fig. 2), and lead us to rely on TEX_{86} temperatures only in the lacustrine sediment preserved in the core, dating from 15.2 ka to 1 ka. The remainder of this paper will focus only on the proxy records from sediments deposited after the Late Pleistocene desiccation of Lake Victoria, with a sampling interval ~200 years.

Above the paleosols, Lake Victoria TEX_{86} temperatures fluctuate ~6 °C, ranging from ~19 °C at ~15.2 ka to ~25 °C at 9 ka (Fig. 3).

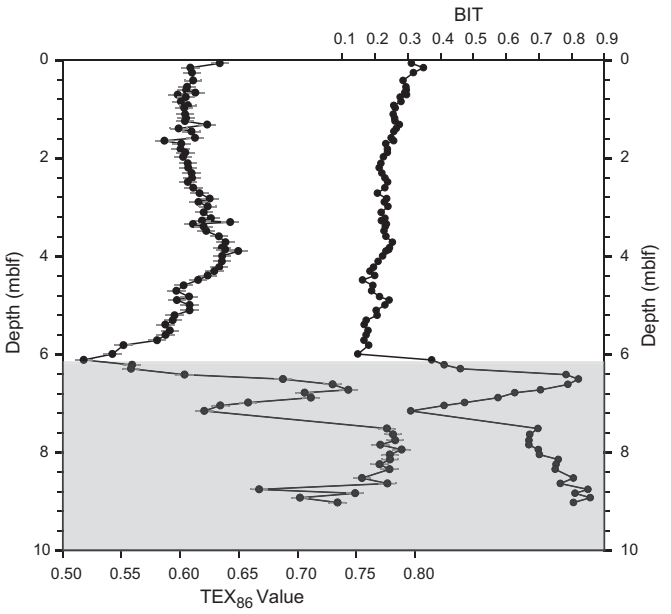

Fig. 2. Down-core records of TEX_{86} and reconstructed lake temperatures and the BIT Index from Lake Victoria plotted versus depth in meters below lake floor (mblf). Prior to ~15.2 ka, BIT Index values are generally higher than ~0.35, suggesting significant terrestrial soil input (shaded region). This substantial soil influence precludes the use of the TEX_{86} as a paleothermometer prior to 15.2 ka and supports previous paleosol interpretation of this portion of the core (Johnson et al., 1996; Johnson et al., 2000). Error bars (gray lines) indicate pooled mean error for a large number of TEX_{86} replicates from East African lakes as described in the method section.

The TEX_{86} record indicates a gradual warming from the late Pleistocene to ~9 ka, with a brief pause between ~12.5 and 11.4 ka interrupting the warming trend. There is a general plateau in warming centered at ~9 ka, followed by a gradual decrease in temperatures from the early to mid-Holocene. This gradual cooling of ~2.5 °C ends during an interval centered on 4.5–4 ka, reaching the lowest temperatures of the Holocene, ~4 °C warmer than the Pleistocene TEX_{86} minimum. The temperatures gradually increase by an average of ~0.5 °C for the remainder of the record.

4.2. The $\delta^{13}C$ n-alkane record

The $\delta^{13}C$ record relies on the values of the C_{29} *n*-alkane, the second most abundant homolog in the Lake Victoria sediments, which showed a trend similar to other measured long chain *n*-alkanes. Reliable analysis of C_{31}, the most abundant homolog, was hindered by the co-elution of another compound, thus giving much larger error bars (though similar trends), while C_{33} (the third most abundant homolog) contains a similar trend to C_{29} described here. The $\delta^{13}C$ data display a range from −23‰ to −27‰, with no significant long term trend throughout the record (Fig. 4). We observe the most stable portions of the record, containing the least $\delta^{13}C$ variability, during the late Pleistocene (~14–12 ka) and middle Holocene (~7–4.7 ka). There are two intervals which deviate from the overall trend, with excursions of as much as 4‰ ^{13}C-depletion from 10 to 8 ka and from ~4.7 to 2.6 ka.

4.3. The δD FAME record

The ice volume corrected δD record of the C_{28} fatty acid from Lake Victoria (Fig. 3) shows a ~35‰ isotopic change, ranging from the most D-enriched values ~−90‰ in the late Holocene to the most D-depleted values, ~−128‰ at 10.8 ka (Fig. 3). D-depletion occurs from ~15 ka until ~12.8 ka, where the record shows a brief reversal of this trend, with D-enrichment of 9‰ until 11.4 ka. This is followed by the most abrupt shift to depleted values of δD in the entire record, ~23‰ in 600 years. Much of the rest of the δD history of the basin is composed of a gradual D-enrichment trend throughout the mid – late Holocene, reaching the most D-enriched values of this record (~90‰) between 4.7 and 2 ka, after which the trend is reversed toward more D-depleted values.

5. Interpretation and discussion

5.1. Interpretation of δD at Lake Victoria as a signal of precipitation amount

We interpret the δD of leaf wax as a proxy of rainfall amount in the Lake Victoria basin. While the primary influences on the isotopic composition of rainfall have been attributed to temperature, latitude, evaporation, rainfall amount, altitude, and continental effects (Dansgaard, 1964), only amount, altitude and continental effects have significant importance at low latitudes (Rozanski et al., 1993; Levin et al., 2009). The influence of temperature on δD of precipitation is considered negligible in the tropics (Rozanski et al., 1993). The magnitude of temperature change seen in the Victoria record (~6 °C) could only account for the kinetic fractionation of <10‰ δD (Majoube, 1971), far less than the almost 40‰ change observed in Lake Victoria sediment core. Relative humidity of the air can potentially influence the δD of leaf wax. Tierney et al. (2011) provides a convincing argument for humidity having minor impact on the δD record from a sediment core from Lake Challa, Tanzania. It is even less likely that changes in relative humidity at Lake Victoria played a major role in the δD observed. Relative humidity today fluctuates between daily highs of ~95%

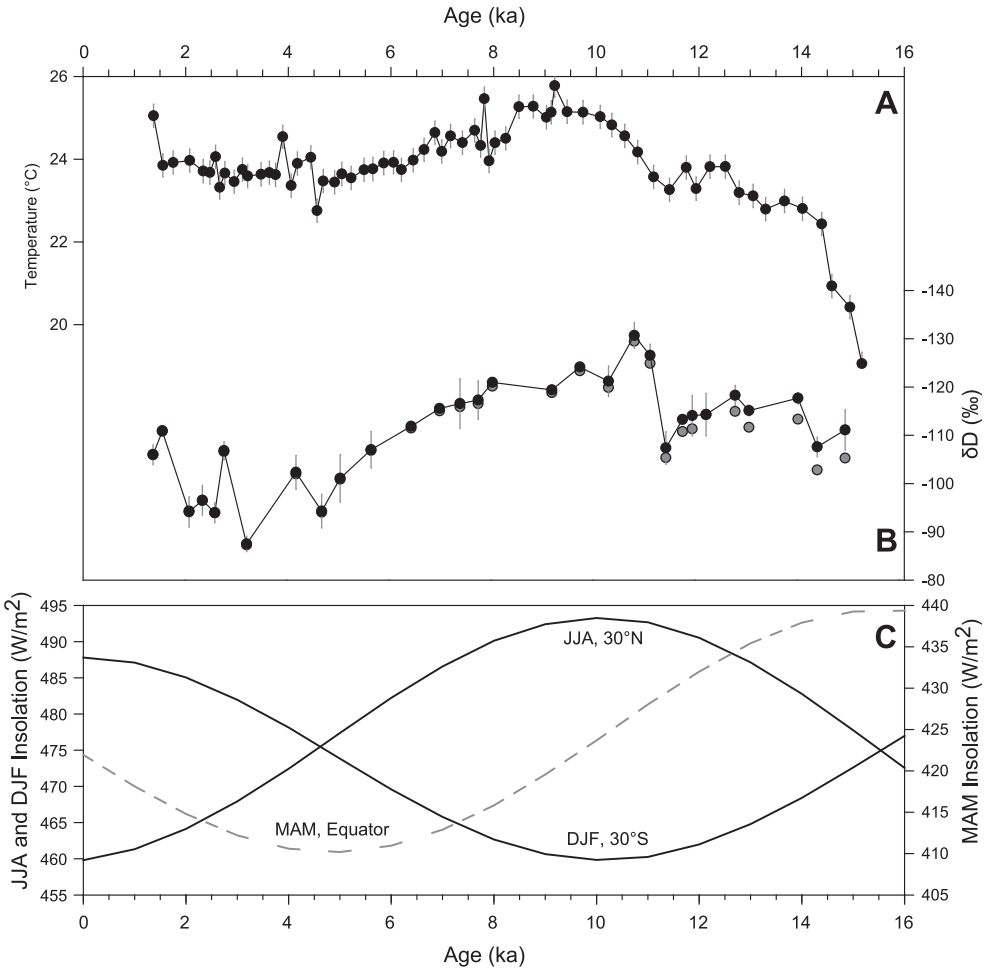

Fig. 3. (A) TEX_{86} paleotemperatures and (B) δD of the C_{29} leaf wax fatty acid methyl ester (FAME) with ice volume δD corrected (black circles) and uncorrected δD (gray circles) shown. Error bars (gray lines) are mean error of replicated analyses for each sample (δD) or pooled mean error for a large number of replicates from East African lakes (TEX_{86}), with an error bar smaller than the symbol in some instances. (C) Insolation curves for June–July–August (JJA) and December–January–February (DJF), showing seasonal contrast between Northern (30°N) and Southern (30°S) Hemispheres. March–April–May (MAM) is presently the season of maximum precipitation delivery to Lake Victoria; MAM insolation at the equator is depicted by the dashed line.

and lows of ~75% at Entebbe, Uganda on the shoreline of Lake Victoria (Kalnay et al., 1996). Hou et al. (2008) found ~10‰ decrease in apparent fractionation for each ~20% increase in humidity from a recent transect study. It is unlikely that there was more than ~5–10% higher humidity in the Victoria basin in the early Holocene compared to its already high range of values today, and this would yield just a 5‰ shift in δD, again, much smaller than the observed range of 40‰ in the Victoria record.

Leaf wax δD has been utilized in a variety of different proxy capacities in previous paleoclimate studies around Africa, depending on the precise location and timescale of interest. The most commonly cited interpretations of the δD proxy in Africa is one of precipitation amount (Schefuß et al., 2005; Tierney et al., 2008; Niedermeyer et al., 2010), moisture source variability (Konecky et al., 2011), and monsoonal intensity (Tierney et al., 2011). Moisture source is likely to have remained consistently from the Indian Ocean at Lake Victoria (Rozanski et al., 1996). The CAB's eastward migration is very likely limited to the rift mountains to the west of Lake Victoria. And given its equatorial setting, the lake is likely to have always had a twice annual passage of the ITCZ, keeping a bimodal rainfall pattern (Verschuren et al., 2009). Lake Victoria is too far removed from the effects of the South African air masses that can influence Lake Malawi (Konecky et al., 2011). Lastly, while there may be minor influence from Indian Monsoonal intensity and factors related to the atmospheric convection of moisture to Lake Victoria (Tierney et al., 2011), we conclude that rainfall amount is the primary control on δD at Lake Victoria because of the strong agreement with pollen records and coincidence with known arid events in East Africa, as further discussed in Section 5.4.

5.2. Precipitation and temperature trends from Lake Victoria and around tropical Africa

The molecular and isotopic records from Lake Victoria indicate a fairly coherent history of hydroclimate and temperature, consistent with theorized linkages in the African tropics (Jolly et al., 1998). Warm and wet conditions prevail in the early Holocene, peaking at ~10–9 ka, with cool, drier conditions in the late Holocene, centered on ~4–3.5 ka. The hydrologic implications of our molecular analyses are generally consistent with past studies of Lake Victoria. Early model results first suggested 20% more precipitation at 9 ka than at present for Lake Victoria, in keeping with the direction and magnitude of Holocene shift seen in the δD record and other Precipitation:Evaporation (P:E) estimates (Hastenrath and Kutzbach, 1983). A diatom-inferred moisture balance also suggests a high lake level between 11 and 8 ka for Lake Victoria (Stager and Mayewski, 1997). Furthermore, Beuning et al.

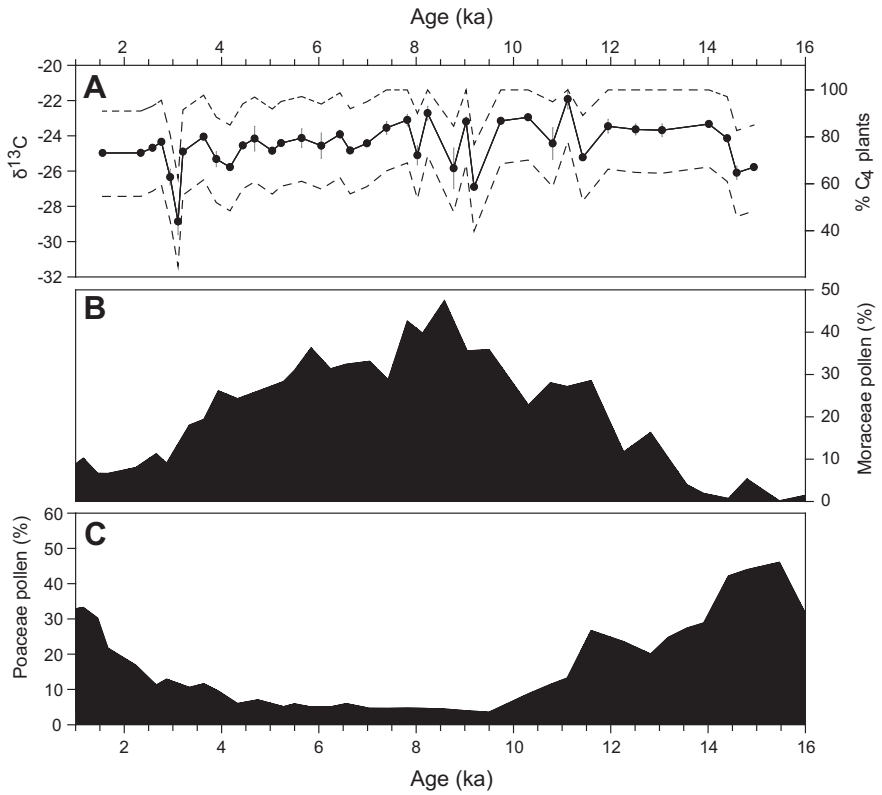

Fig. 4. Comparison between the molecular vegetation proxy record, $\delta^{13}C$, and a previously published pollen record from northern Lake Victoria (Kendall, 1969): (A) $\delta^{13}C$ of C_{29} *n*-alkane, with error bars (gray lines) that indicate the mean error of replicate analyses. The percentage of C_4 plants, as estimated using a two end member mixing model is shown on the right axis, with dashed lines that represent one standard deviation from the C_4 plant percentage estimate, as determined using $\delta^{13}C$ from literature documented values of C_3 and C_4 plants (Castañeda et al., 2009b); (B) the relative abundance of Moraceae (trees/shrubs) and (C) Poaceae (grasses), the two most abundant pollen types at Lake Victoria.

(1997b, 2002) estimated lake water $\delta^{18}O$ from aquatic cellulose in nearby Lake Victoria sediment cores and found a shift to more ^{18}O-depleted values during the early Holocene and ^{18}O-enrichment during the late Pleistocene, interpreted as a response to wetter and more arid conditions, respectively. These results are consistent with the timing of δD-inferred high precipitation during the early–mid Holocene (Fig. 5).

The early–mid Holocene high precipitation interval at Lake Victoria aligns with a well-documented wet period throughout North Africa and the equatorial tropics (Gasse, 2000). For instance, Lake Kivu, another equatorial lake near Lake Victoria, experienced high lake levels during the early Holocene (Gasse, 2000), concomitant with increased precipitation in the Lake Victoria region. Recent investigations of leaf wax δD in the sediments of Lake Challa (Tierney et al., 2011) and Lake Tanganyika (Tierney et al., 2008) are generally consistent with prior estimates of water balance in these lakes (Gasse et al., 1989; Beuning et al., 1997a) and the Lake Victoria record of δD (Fig. 5). Lake Challa is the most proximal δD record to Lake Victoria, and it captures a similar overall hydroclimate pattern, interpreted to be a proxy for the East African Monsoon (EAM) intensity, though with minor offsets in timing between events seen in this record and Lake Victoria and with an early–mid Holocene that does not show as clear a record of progressive D-enrichment (Tierney et al., 2011). Similarly, this pattern extends to central West Africa where coeval shifts between wet and dry periods occurred in the Congo Basin (Schefuß et al., 2005). A record of δD from a marine sediment core taken off the west coast of the African Sahel shows broadly consistent hydroclimate patterns with Lake Victoria until ~8 ka (Niedermeyer et al., 2010). A δD record from in the Mozambique Channel draining the Zambezi River has a wetter interval during the YD, indicating δD is likely controlled by a southward shift of the ITCZ during Northern Hemisphere cold events (Schefuß et al., 2011). The magnitude of isotopic shift seen in the Lake Victoria δD record is also in keeping with other records of leaf wax δD in tropical Africa during latest Pleistocene–Holocene, a significant ~30–40‰ change (Schefuß et al., 2005; Tierney et al., 2008; Konecky et al., 2011; Tierney et al., 2011).

Hydroclimate results from Lake Victoria do not appear to closely match those from Lake Malawi (Fig. 5). Cumulative results suggest that the climate behavior of Lake Malawi during the Holocene was anti-phased with much of the rest of tropical Africa, presumably due its more southerly position (Barker and Gasse, 2003). Various lines of evidence including sediment composition (Finney et al., 1996), pollen (DeBusk, 1998) and *n*-alkane $\delta^{13}C$ (Castañeda et al., 2007) indicate a drier early Holocene when compared to the Late Holocene at the Lake Malawi basin in phase with cool temperatures. Additionally, the δD record from Lake Malawi (Fig. 5) is not consistent with the history of rainfall amount inferred from the $\delta^{13}C$ record of *n*-alkanes, however, but instead reflects a complex history of shifting atmospheric circulation patterns and sources of moisture (Konecky et al., 2011).

TEX_{86} temperature reconstructions from Lake Victoria (this study), Lake Malawi (Powers et al., 2005), Lake Tanganyika (Tierney et al., 2008) and an MBT/CBT record from the Congo Basin (Weijers et al., 2007) spanning this interval indicate temperatures are not as consistent as rainfall records in tropical Africa (Fig. 6). While inter-lake comparisons of absolute temperature are tentative due to their individual calibrations of TEX_{86} to temperature, the temperature of Lake Victoria appears to be significantly cooler than Lake

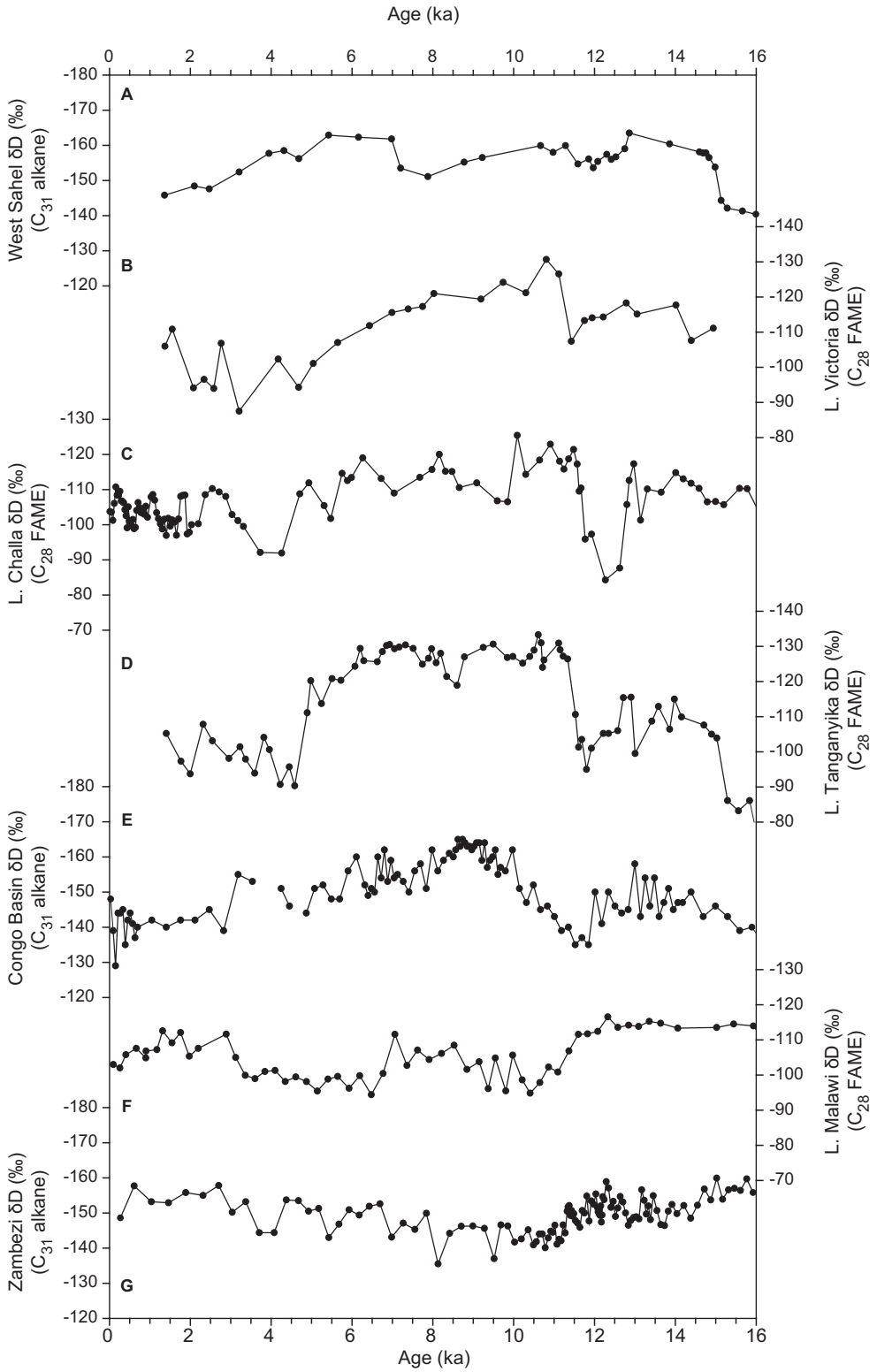

Fig. 5. Comparison of African compound specific δD records with the compound analyzed for each record: (A) West Sahel/Senegal River drainage (GeoB9508-5) (Niedermeyer et al., 2010); (B) Lake Victoria δD of C_{28} FAME (this study); (C) Lake Challa of C_{28} FAME (Tierney et al., 2011); (D) Lake Tanganyika δD of C_{28} FAME (Tierney et al., 2008); (E) Congo Basin (central West Africa) δD of C_{29} *n*-alkane (Schefuß et al., 2005); (F) Lake Malawi δD of C_{28} FAME (Konecky et al., 2011); (G) Zambezi River catchment (GeoB9307-3) (Schefuß et al., 2011).

Tanganyika or Lake Malawi at 15 ka, perhaps because of its higher elevation (1133 m above sea level (masl) for Victoria versus 773 and 437 masl, respectively, for the other two lakes). The Congo Basin record is one of gradual warming throughout the Late Pleistocene and Holocene, and the Lake Tanganyika history of temperature displays maximum warmth around 10 ka and around 5–6 ka, with brief excursions to warm temperatures at about 11.5 ka and 7 ka. The TEX_{86} temperature record from Lake Malawi at the southern

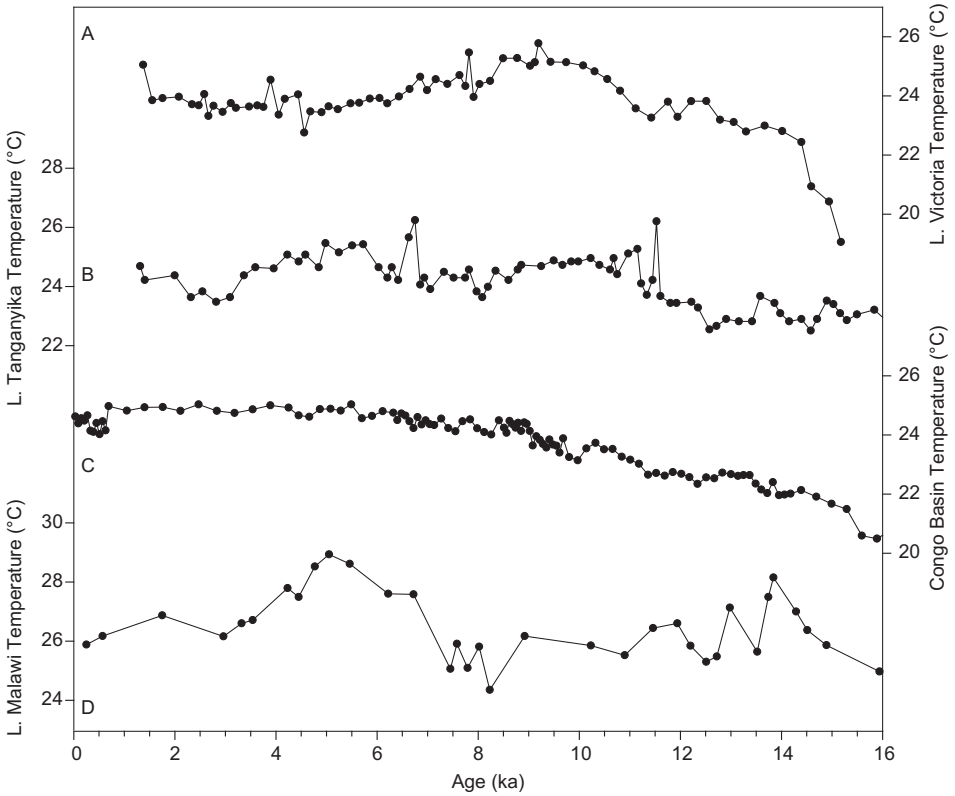

Fig. 6. Molecular paleotemperature records from Africa: (A) Lake Victoria TEX_{86} temperatures (this study); (B) Lake Tanganyika TEX_{86} temperatures (Tierney et al., 2008); (C) Congo Basin (central West Africa) Methylation index of Branched Tetraethers (MBT) mean annual air temperature (Weijers et al., 2007); (D) Lake Malawi TEX_{86} temperatures (Powers et al., 2005).

extent of the East African Rift Valley exhibits trends strongly contrasting with the record from Lake Victoria, with a relatively cool early Holocene and the warmest conditions centered at 5 ka (Powers et al., 2005).

The warm and sustained high precipitation interval during the early Holocene, followed by a gradual end to these conditions into the late Holocene likely reflects the end of the African Humid Period (AHP), the magnitude and timing of which were transgressive across Africa. The AHP (~14.5–5.5 ka) was a humid interval documented around much of North and East Africa, in some cases terminating in an abrupt shift to arid conditions (deMenocal et al., 2000) and in other cases, a more gradual shift (Niedermeyer et al., 2010; Vincens et al., 2010). While Lake Victoria δD and TEX_{86} indicates a gradual shift to drier, cooler conditions until the late Holocene, other African locations show similar conditions developing, but with varied timing. While the absolute age from an ice core from Mt. Kilimanjaro is debated, it is interesting to note that it contains a thick dust layer ~4 ka, interpreted to be from sizable dust storms due to regionally extensive aridity (Thompson et al., 2002). This dust signal is also found in the eastern Mediterranean and in the Gulf of Oman (Dalfes et al., 1997; Magny et al., 2009). Low lake levels and nitrogen isotopic composition of bulk organic matter indicate a laterally continuous transect of dry conditions around tropical Africa, from records at Lake Bosumtwi, Ghana (Talbot et al., 1984; Russell et al., 2003) to Lake Abhé in Ethiopia (Gasse, 1977). Lake Tanganyika shows significant cooling at 3.6–2 ka, but pronounced drying took place earlier, at ~5 ka (Tierney et al., 2008). Berke et al. (2012) highlights a regional warming of varying magnitude within temperature records from Lakes Turkana, Tanganyika (Tierney et al., 2008), and Malawi (Powers et al., 2005), which is manifested in the ice core $\delta^{18}O$ record from Mt. Kilimanjaro as well (Thompson et al., 2002). While Lake Victoria indicates a gradual climate shift during the Holocene, there is no associated excursion to warmer conditions near the end of the AHP as seen in other TEX_{86} records.

Just as Lake Victoria is anomalous in its lack of maximum Holocene temperature ~5 ka, it also displays far less response to the Younger Dryas (YD) cold period ~12.5–11.8 ka than other East African lakes. There appears to be a subtle thermal and hydrological response recorded in Lake Victoria during the YD, which is more pronounced elsewhere around tropical East Africa (Castañeda et al., 2007; Talbot et al., 2007; Gasse et al., 2008; Verschuren et al., 2009; Sinninghe Damsté et al., 2011; Tierney et al., 2011). The records at Lake Victoria display a pause or slight reversal in the trends of warming and D-depletion between 12.2 ka and 11.4 ka, which likely coincide with the YD, given the range of uncertainty in radiocarbon chronology. While subtle, the Victoria YD signal is reflected more in the δD than in the TEX_{86} profile, as is the case for Lake Tanganyika (Figs. 6 and 7) (Tierney et al., 2008). Following the termination of the YD, there is a significant shift to warmer, wetter conditions at Lake Victoria.

5.3. Terrestrial vegetation response to climate changes at Lake Victoria

The shifts in $\delta^{13}C$ do not appear to vary coherently and suggest changes in climate are having little effect on the balance between C_3 and C_4 plants that is being recorded by *n*-alkanes in the sediments of the Victoria basin (Fig. 4). A simplified two-end member mixing model is applied to the $\delta^{13}C$ data to estimate the relative contributions of C_4 and C_3 plants, using the C_{29} *n*-alkane abundances and assuming average $\delta^{13}C$ values of −21.4‰ and −34.7‰, respectively (Collister et al., 1994; Castañeda et al., 2009b). Based on this estimation, the Lake Victoria region has a C_4-dominated

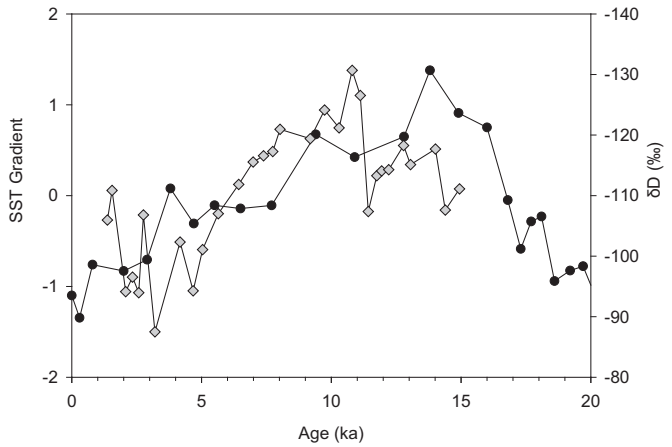

Fig. 7. Indian Ocean SST west–east (W–E) gradient (black circles) determined using alkenone SSTs from the eastern Indian Ocean (Mohtadi et al., 2010) and western Indian Ocean (Bard et al., 1997). Lake Victoria leaf wax δD shown for comparison (gray diamonds).

(~70–90%) landscape throughout the latest Pleistocene and Holocene (Fig. 4). There is significant uncertainty associated with the percentage of C_4 plants estimated using the simple mixing model (Fig. 4). Using the standard deviation for *n*-alkane $\delta^{13}C$ of C_3 and C_4 plants, the largest of which is 2.6‰ (Castañeda et al., 2009b), there is an associated error in percentage of C_4 plants of ±20%.

The $\delta^{13}C$ record provides few clues as to the changes occurring in the terrestrial ecosystem surrounding Lake Victoria, while the pollen records of Kendall (1969) and Beuning (1999) provide ample evidence of changing vegetation that accompanied the climate history in this region (Fig. 4). The percentage of moist forest (tree/shrub) pollen (Moraceae, Urticaceae, Alchornea, Macaranga, and Trema), composed overwhelmingly of Moraceae, indicates a record-maximum of 66% humid species pollen at 8.6 ka (Stager et al., 2003), which correlates well to the warm, D-depleted interval described here. Low abundances of Poaceae (grass) pollen occur throughout this interval, as might be expected if the majority of these grasses are C_4. Previous research indicates that the overwhelming majority (>90%) of modern grasses in East Africa are C_4 grasses (Livingstone and Clayton, 1980; White, 1983). Cyperaceae (sedges), the second most abundant C_4 plant group globally, could influence the $\delta^{13}C$ record. However, low fossil Cyperaceae pollen abundances at Lake Victoria roughly align with the low fossil Poaceae pollen abundances (Kendall, 1969) and periods of relative D-depletion. Although there are some semi-aquatic C_3 Cyperaceae species found in Africa, high Cyperaceae abundance has been linked to prograding shoreline and swamps due to increased aridity (Kendall, 1969; Gasse and Van Campo, 1994), which would agree well with our interpretation of this interval.

There are relatively few studies that focus on both pollen and lipid $\delta^{13}C$ results to reconstruct vegetation changes and in those studies that have attempted a correlation, it is often noted that a close match between records might not be seen in light of the differences in production, transport, supply, and deposition of lipids and pollen. Niedermeyer et al. (2010) found $\delta^{13}C$ of leaf waxes from a marine core off the northwest coast of Africa that did not vary with large shifts in δD of leaf waxes and attributed this response to a change in seasonality of rainfall, where a drier rainy season was not enough to support C_3 vegetation. This interpretation does not appear to be supported at Lake Victoria based on the pollen evidence available. However, we can envision a few possible hypotheses to explain these puzzling results. Firstly, there may be potential bias inherent in pollen or $\delta^{13}C$ *n*-alkane records being sourced from the same region. Pollen results can be skewed toward plants producing larger amounts of pollen, those plants not toward the edge of their reproductive viability or toward those pollinated by the wind, while some are clonal, with delayed pollen production (Prentice and Webb, 1986). Similarly, leaf wax results can be skewed, due to varied homolog distributions and $\delta^{13}C$ of different plant species (Rommerskirchen et al., 2006; Vogts et al., 2009; Diefendorf et al., 2011) as well as varying proclivity toward wax melt and abrasion of specific *n*-alkane homologs (Rommerskirchen et al., 2003). Additionally, there is evidence of large differences in the timing of leaf wax synthesis for grasses, which show continuous annual production (Smith and Freeman, 2006; Sachse et al., 2010), and trees, with a finite annual production (Mortazavi et al., 2009; Kahmen et al., 2011), which is likely to alter input to the sediments. Further, transport of leaf waxes has been shown to be size fraction-dependent, with C_4-derived carbon preferentially incorporated into the finer transported fraction, and therefore likely to travel farther distances than the C_3-derived carbon associated with coarser transported fraction (Bird and Pousai, 1997). However, the argument that pollen and lipid wax results are recording different source regions must also be considered. Farrimond and Flanagan (1996) found inconsistency between pollen and lipid records and suggested that this was due to lipids recording a more local signal of immediate vegetation while pollen represented a wider, regional assemblage. Still and Powell (2010) analyzed vegetation patterns using MODIS Vegetation Continuous Fields (VCF) maps generated for Africa and found that the majority of modern vegetation around Lake Victoria is C_3 (~90–100%), while the southeastern portion of the region is dominated by C_4 plants (~75–100%). We speculate that within the constraints of the spatial resolution of this MODIS VCF map, the generally southeasterly winds (Levin et al., 2009) over the lake may preferentially move leaf waxes from the C_4 dominated landscape into the basin while pollen in this environment may provide a more regional vegetation perspective, though further analyses are needed to support this claim. Thus, while pollen percentages have non-linear relationships with vegetation abundance, and cannot be directly related to species abundances or biomass (Prentice and Webb, 1986), the similar trends of pollen and hydroclimate at Lake Victoria support the use of pollen as a regional vegetation proxy, while there is no straightforward relationship between $\delta^{13}C$ and regional vegetation around Lake Victoria.

5.4. *Possible controls on δD beyond those of regional aridity at Lake Victoria*

Comparison of δD from Lake Victoria with the history of regional aridity from lake level indicators (Gasse, 2000; Gasse et al., 2008) demonstrates striking similarities, and suggests that δD reflects changes in moisture balance in the area. But another potentially significant control on δD is the variation in the magnitude of D/H fractionation by different vegetation types. We observe a strong parallel trend in the pollen and δD records in Lake Victoria, albeit without an accompanying trend in $\delta^{13}C$ of the plant leaf waxes. This raises the question of whether the δD record of core V95-1P is mainly due to the effects of changes in rainfall or vegetation. We interpret the δD record as one of rainfall, partly because the shifts in δD, such as at 11.4 ka, do not align precisely with shifts in the dominant pollen. In addition, recent studies have shown that the difference in apparent fractionation of δD between C_3 trees and C_4 grasses may in fact be small, or perhaps negligible (Tierney et al., 2010). Hou et al. (2008) found that a greenhouse grown C_4 grass (*Zea mays*) had an apparent fractionation of -127 ± 6‰ for the C_{28} fatty acid, while C_3 trees showed less apparent fractionation, $\sim -114 \pm 8$‰ for the C_{28} fatty acid. Furthermore, the integrated apparent fractionation signal of δD in plant leaf waxes appears to be

relatively constant along field transects of widely varied vegetation types, both in Europe (Sachse et al., 2004; Hou et al., 2008) and in the southwestern USA (Hou et al., 2008). A transect of surface sediments from lakes across Cameroon (west Central Africa) found that δD of long chain *n*-alkanes served well as a proxy of regional source water, and that changes between C_3 and C_4 photosynthetic pathway could not explain variations seen in δD (Garcin et al., 2012). In Lake Victoria, as illustrated by pollen analyses, our δD record spans changes from a Moraceae-dominated (C_3 trees/shrubs) landscape to a Poaceae-dominated (C_4 grasses) landscape. If δD were an artifact of vegetation changes, a shift to a C_3 tree-dominated environment, such as during the early–mid Holocene at Lake Victoria, would reduce the apparent fractionation, shifting to less D-depleted values, which is not seen. These results support the independence of δD from vegetation changes in this record. We therefore attribute primary control on the variability in δD seen at Lake Victoria to changes in the regional hydroclimate, with little influence by changes in terrestrial vegetation.

6. Possible climate controls and implications

6.1. Insolation and ENSO forcing at Lake Victoria

There is a long-standing debate regarding the relative input of Indian versus Atlantic Ocean moisture to East African lakes on millennial time scales. Atlantic Ocean moisture arrives in East Africa after being recycled through the West African Congo Basin (Schefuß et al., 2003). Oceanic moisture is transported by either the West African or Indian monsoon system, whose relative contribution is determined in large part by the movement of the CAB, system strength, and topography (Nicholson, 1996; Levin et al., 2009). Modern isotopic studies of meteoric waters and remote radar precipitation data indicate that strong easterly to southeasterly winds bring rainfall to Kenya, and implicate the Indian Ocean as the primary supply of Lake Victoria moisture (Levin et al., 2009). This supports previous investigations which found strong connections between Indian Ocean zonal atmospheric circulation and the level of Lake Victoria (Bergonzini et al., 2004) and between East African rainfall anomalies and western Indian Ocean SST and the atmospheric jet (Hastenrath et al., 1993). Although we note similarities between the record of rainfall presented here and that from the Congo Basin (Schefuß et al., 2005) (Fig. 5), we believe the evidence implicates a western Indian Ocean moisture source. The CAB does not transit Lake Victoria at the present time, according to NCEP reanalysis of 925 h Pa mean winds (Levin et al., 2009), due to the orography of the western arm of the rift valley, and likely did not shift significantly over the interval described here (Nicholson, 1996; Levin et al., 2009).

The history of rainfall and temperature in the Lake Victoria basin, as reflected in the records of TEX_{86} and δD, is roughly in-phase with June–July–August (JJA) insolation (Fig. 3) and points to the strong role of insolation on tropical climate. The interval of increased moisture balance shown by D-depletion between 11 and 8 ka is also the time of greatest interhemispheric contrast in summer insolation (JJA and DJF), and we hypothesize that this may be an important factor controlling the climate of the Lake Victoria basin (Fig. 3). At Lake Victoria, the termination of warm, wetter conditions centered on ~4 ka marks the inflection of the JJA insolation curve, suggesting this is perhaps a response to some sort of insolation threshold. Likewise, precipitation delivery peaks at Lake Victoria during MAM (Nicholson, 1996) and the insolation trend shows a minimum for MAM that is coincident with the interval of smallest seasonal contrast between JJA and DJF at ~4 ka, perhaps also weakening moisture generation and delivery. This interpretation is consistent with a climate forcing mechanism proposed by Verschuren et al. (2009) for Lake Challa, another near-equatorial African lake. Interhemispheric seasonal insolation gradients between boreal summer (June) and austral summer (December) were linked to the BIT Index in Lake Challa sediment, used as a proxy for precipitation-induced runoff (Verschuren et al., 2009). According to these authors, orbitally-induced insolation variability would lead to increased NE or SE trade winds bearing moisture off the Indian Ocean. A reduction in rainfall occurs when the contrast between seasonal hemispheric insolation gradients reach a minimum, corresponding to a period lacking heightened monsoonal activity and an abatement of local trade winds (Verschuren et al., 2009). Modeling studies support the linkage between variations in tropical precipitation amount on long time scales to insolation-controlled monsoonal moisture fluxes (Abram et al., 2007; Tjallingii et al., 2008). Beyond the insolation contrasts already discussed, the October–November–December insolation (OND) is at a minimum ~4 ka when MAM is at a maximum. Today these short rains express 50–70% of the interannual variability, more than the long rains of MAM (Nicholson, 1996), but this may not have necessarily been the case for the last 25 ka (Verschuren et al., 2009). Additionally, when the OND insolation reached a maximum at ~16 ka, other factors, including recovery following Heinrich 1 (H1), left much of Africa, including the Lake Victoria region, dry.

The conditions described at Lake Victoria may involve the dynamics of the Indian Ocean Dipole (IOD) (Saji et al., 1999; Abram et al., 2007). The IOD is a coupled ocean-atmosphere phenomenon based on temperature gradients in the Indian Ocean (Abram et al., 2007). The positive IOD mode exhibits relatively warm temperatures in the western Indian Ocean, an intensification of atmospheric convergence over East Africa, and an increased monsoonal intensity (Saji et al., 1999), conditions that broadly match the early to mid-Holocene of Lake Victoria. Previous modeling studies have found that the early–mid Holocene was an interval of enhanced cooling in the eastern Indian Ocean, leading to more positive IOD events (Abram et al., 2007, 2009). The positive IOD mean state is linked to strengthened monsoon winds creating upwelling in the eastern Indian Ocean from enhanced easterly zonal winds at the equator (Abram et al., 2009). Additionally, model results have shown a positive feedback during positive IOD-like events, with SST gradients across the Indian Ocean resulting from insolation-driven monsoonal intensification (Liu et al., 2003; Abram et al., 2007; Krishnan and Swapna, 2009).

In order to assess the possible influence of an Indian Ocean SST gradient on the Lake Victoria hydroclimate through time, we used marine alkenone temperature reconstructions from the eastern Indian Ocean (Mohtadi et al., 2010) and western Indian Ocean (Bard et al., 1997) in order to determine the west–east (W–E) temperature gradient (Fig. 7). We note that the SST gradient increases from the Last Glacial Maximum, ~21 ka, until around the time of the Bølling–Allerød (~14 ka). Assuming the Indian Ocean SST gradient contributes to the strength of the East African monsoon, we note strong agreement between a peak in the SST gradient, and refilling of Lake Victoria ~15 ka following a complete lake desiccation, which created the paleosols discussed earlier. Further, a δD record from nearby Lake Challa, interpreted as a record of the East African Monsoon (EAM) intensity, shows strong agreement with Lake Victoria δD, specifically indicating that while Lake Victoria was particularly wet in early Holocene, the EAM was strong, driving moisture landward to this region (Tierney et al., 2011). Following the strong positive W–E SST gradient (Fig. 7) and wet conditions at Lake Victoria, a steady decrease in the SST gradient is observed, with a steeper decrease noted at the H1 and the YD events, coincident with arid conditions at Lake Victoria.

Insolation-driven warming and increased moisture due to both insolation and the positive IOD seem to have been interrupted at

Lake Victoria during the YD, as evidenced by a pause in increasing temperatures and rainfall, as well as dramatic cooling and drying elsewhere in East Africa. The shifting of the mean ITCZ position is often called upon to explain paleohydrological changes around Africa in regions where it prominently influences modern climate, particularly at the northern and southern extents of its modern pathway (Johnson et al., 2002; Schefuß et al., 2011). It has been proposed that the YD climate anomaly was caused by the reduction or complete shutdown of Atlantic Meridional Overturning Circulation (AMOC) originating in the North Atlantic from a large freshwater input (Broecker et al., 1989). While modeling results (Chang et al., 2008; Chiang et al., 2008) and paleoclimate records (Castañeda et al., 2007; Tjallingii et al., 2008; Schefuß et al., 2011) suggest that an AMOC reduction would likely displace the ITCZ to the south and thus dramatically shift the distribution of rainfall around Africa, it is unlikely that this shift would have a significant impact on the moisture balance at Lake Victoria. The equatorial position of Lake Victoria ensures that a southward displacement of the ITCZ could not have been shifted so far as to prevent the twice annual migration across Lake Victoria although it is likely it was skewed a bit to the south of its present seasonal migration.

The AMOC slowdown was likely communicated to East Africa by the ocean–atmosphere climate dynamics of the El Niño Southern Oscillation (ENSO) (Chiang, 2009). Observational studies and modeling simulations have shown that ENSO dynamics are linked to the precipitation patterns in East Africa, specifically during arid East African La Niña events (Camberlin, 1997; Nicholson and Selato, 2000; Camberlin and Philippon, 2002). Perhaps the strongest connection between ENSO and the deglacial AMOC was found using a suite of coupled general circulation models (CGCMs), which found that the tropical Pacific mean state and ENSO variability showed significant response to a weakening of the AMOC (Timmermann et al., 2005, 2007). Freshwater forcing in the North Atlantic established a meridional Atlantic Ocean temperature gradient, ultimately leading to ENSO intensification, expressed as the cooling of the northeastern tropical Pacific (La Niña-like conditions) (Timmermann et al., 2007). Alternatively, modeling simulations of Clement et al. (2001) indicate that La Niña-like SSTs can lock into the tropical Pacific as an abrupt response to gradual change in orbital forcing when the Earth is in perihelion during boreal winter or summer, mimicking the timing and conditions of the Younger Dryas without calling upon major freshwater hosing of the North Atlantic from a melting ice sheet. By either mechanism, La Niña-like SSTs are produced, which would lead to the weakening of the W–E gradient in Indian Ocean SST, as we observe (Fig. 7). A significant reduction in monsoonal moisture to East Africa is seen in the Lake Challa δD with an associated 30‰ δD excursion at the YD (Tierney et al., 2011), consistent with Lake Victoria aridity. The cessation of moisture transport from the Indian Ocean is from reduction of Indian Ocean atmospheric convection and associated reduction in zonal winds, and supported by ocean–atmosphere modeling simulations which have an Atlantic hosing leading to an overall weakened Northern Hemisphere monsoon systems (Dahl et al., 2005; Broccoli et al., 2006). Following the YD and warming in the Northern Hemisphere, reorganization of the tropical monsoonal systems are rapid, as is evidenced in an abrupt resumption of the monsoonal strength as seen in Indian Ocean (Fleitmann et al., 2007) and Asian (Wang et al., 2008) stalagmites, yielding, in the case of Lake Victoria, a more significant shift in δD than the initialization of the YD.

7. Conclusions

The records of δD of leaf waxes and TEX_{86} from Lake Victoria indicate coherence between hydroclimate and temperature during the latest Pleistocene and Holocene and provide evidence of orbitally-forced tropical climate. We observe an increase in warm, wet conditions during the late Pleistocene, peaking in the early Holocene, before gradually cooling and drying to minimum values of temperature and rainfall at ~4.7–3.2 ka. This pattern is in agreement with an early to mid-Holocene high moisture balance and drier, cooler mid-late Holocene following the end of the AHP, temporally transgressive across North and East Africa. We observe relatively modest changes in the record of $\delta^{13}C$ of plant leaf wax compounds, while fossil pollen suggests significant change in the terrestrial vegetation, shifting from theorized abundant C_3 trees and shrubs (dominated by Moraceae) during the warm, wet interval of the mid-Holocene, to C_4 grasses (Poaceae) during cooler, drier intervals of the latest Pleistocene and late Holocene. The Lake Victoria record of temperature and precipitation amount is consistent with the concept of the influence of the seasonal contrast between JJA and DJF in the Northern and Southern Hemisphere insolation on equatorial rainfall, with enhanced delivery of monsoonally-derived precipitation when the contrast is at a maximum. The communication of climate events such as the YD to Lake Victoria and other East African locales may indicate an added forcing mechanism, with ENSO dynamics overprinting the gradual insolation forcing.

Acknowledgments

We thank LacCore, the National Repository for Lake Sediment Cores at the University of Minnesota for core access and assistance. We thank Ellen Hopmans, Jort Ossebaar, Sarah Grosshuesch, and Julia Halbur for assistance. This research was funded by grant NA-060-AR4310113 from the U.S. Department of Commerce, National Oceanic and Atmospheric Administration. The research leading to these results has received funding from the European Research Council under the European Union's Seventh Framework Programme (FP7/2007–2013)/ERC grant agreement n° [226600]. Support from the Gledden Fellowship to J.P.W. and European Association of Organic Geochemists to M.A.B. is acknowledged. Work prepared while J.P.W. on leave at the Centre for Water Research, University of Western Australia and the WA-Organic & Isotope Geochemistry Centre, Curtin University of Technology. This work forms contribution 2641-JW at the Centre for Water Research, The University of Western Australia.

References

Abram, N.J., Gagan, M.K., Liu, Z., Hantoro, W.S., McCulloch, M.T., Suwargadi, B.W., 2007. Seasonal characteristics of the Indian Ocean Dipole during the Holocene epoch. Nature 445, 299–302.

Abram, N.J., McGregor, H.V., Gagan, M.K., Hantoro, W.S., Suwargadi, B.W., 2009. Oscillations in the southern extent of the Indo-Pacific Warm Pool during the mid-Holocene. Quat. Sci. Rev. 28, 2794–2803.

Bard, E., Rostek, F., Sonzogni, C., 1997. Interhemispheric synchrony of the last deglaciation inferred from alkenone palaeothermometry. Nature 385, 707–710.

Barker, P., Gasse, F., 2003. New evidence for a reduced water balance in East Africa during the Last Glacial Maximum: implication for model-data comparison. Quat. Sci. Rev. 22, 823–837.

Beadle, L.C., 1981. The Inland Waters of Tropical Africa: an Introduction to Tropical Limnology. Longman, London.

Bergonzini, L., Richard, Y., Petit, L., Camberlin, P., 2004. Zonal circulations over the Indian and Pacific Oceans and the level of Lakes Victoria and Tanganyika. Int. J. Clim. 24, 1613–1624.

Berke, M.A., Johnson, T.C., Werne, J.P., Schouten, S., Sinninghe Damsté, J.S., 2012. A mid-Holocene thermal maximum at the end of the African Humid Period. Earth Planet. Sci. Lett.

Beuning, K.R., 1999. A re-evaluation of the late glacial and early-Holocene vegetation history of the Lake Victoria region. Palaeoecol. Afr. 26, 115–136.

Beuning, K.R., Talbot, M.R., Kelts, K., 1997a. A revised 30,000-year paleoclimatic and paleohyrdologic history of Lake Albert, East Africa. Palaeogeogr. Palaeoclimatol. Palaeoecol. 136, 259–279.

Beuning, K.R.M., Kelts, K., Ito, E., Johnson, T.C., 1997b. Paleohydrology of Lake Victoria, East Africa, inferred from $^{18}O/^{16}O$ ratios in sediment cellulose. Geology 25, 1083–1086.
Beuning, K.R.M., Kelts, K., Russell, J., Wolfe, B.B., 2002. Reassessment of Lake Victoria–Upper Nile River paleohydrology from oxygen isotope records of lake-sediment cellulose. Geology 30, 559–562.
Bird, M.I., Pousai, P., 1997. Variations of $\delta^{13}C$ in the surface soil organic carbon pool. Global Biogeochem. Cycles 11, 313–322.
Blaga, C., Reichart, G.-J., Heiri, O., Sinninghe Damsté, J., 2009. Tetraether membrane lipid distributions in water-column particulate matter and sediments: a study of 47 European lakes along a north–south transect. J. Paleolimnol. 41, 523–540.
Blaga, C.I., Reichart, G.-J., Vissers, E.W., Lotter, A.F., Anselmetti, F.S., Sinninghe Damsté, J.S., 2011. Seasonal changes in glycerol dialkyl glycerol tetraether concentrations and fluxes in a perialpine lake: implications for the use of the TEX_{86} and BIT proxies. Geochim. Cosmochim. Acta 75, 6416–6428.
Broccoli, A.J., Dahl, K.A., Stouffer, R.J., 2006. Response of the ITCZ to Northern Hemisphere cooling. Geophys. Res. Lett. 33. http://dx.doi.org/10.1029/2005GL024546
Brochier-Armanet, C., Boussau, B., Gribaldo, S., Forterre, P., 2008. Mesophilic crenarchaeota: proposal for a third archaeal phylum, the Thaumarchaeota. Nat. Rev. Microbiol. 6, 245–252.
Broecker, W.S., Kennett, J.P., Flower, B.P., Teller, J.T., Trumbore, S., Bonani, G., Wolfli, W., 1989. Routing of meltwater from the Laurentide Ice Sheet during the Younger Dryas cold episode. Nature 341, 318–321.
Camberlin, P., 1997. Rainfall anomalies in the source region of the Nile and their connection with the Indian summer monsoon. J. Clim. 10, 1380–1392.
Camberlin, P., Philippon, N., 2002. The East African March–May rainy season: associated atmospheric dynamics and predictability over the 1968–97 period. J. Clim. 15, 1002–1019.
Castañeda, I., Werne, J.P., Johnson, T.C., 2009a. Influence of climate change on algal community structure and primary productivity of Lake Malawi (East Africa) from the Last Glacial Maximun to present. Limnol. Oceanogr. 54, 2431–2447.
Castañeda, I.S., Mulitza, S., Schefuß, E., Lopes dos Santos, R.A., Sinninghe Damsté, J.S., Schouten, S., 2009b. Wet phases in the Sahara/Sahel region and human migration patterns in North Africa. PNAS 106, 20159–20163.
Castañeda, I.S., Werne, J., Johnson, T.C., 2007. Wet and arid phases in the southeast African tropics since the Last Glacial Maximum. Geology 35, 823–826.
Cerling, T.E., Harris, J.M., MacFadden, B.J., Leakey, M.G., Quade, J., Eisenmann, V., Ehleringer, J.R., 1997. Global vegetation change through the Miocene/Pliocene boundary. Nature 389, 153–158.
Chang, P., Zhang, R., Hazeleger, W., Wen, C., Wan, X., Ji, L., Haarsma, R.J., Breugem, W.-P., Seidel, H., 2008. Oceanic link between abrupt changes in the North Atlantic Ocean and the African monsoon. Nat. Geosci. 1, 444–448.
Chiang, J.C.H., 2009. The tropics in paleoclimate. Annu. Rev. Earth Planet. Sci. 37, 263–297.
Chiang, J.C.H., Fang, Y., Chang, P., 2008. Interhemispheric thermal gradient and tropical Pacific climate. Geophys. Res. Lett. 35, L14704.
Chikaraishi, Y., Naraoka, H., 2007. $\delta^{13}C$ and δD relationships among three *n*-alkyl compound classes (*n*-alkanoic acid, *n*-alkane and *n*-alkanol) of terrestrial higher plants. Org. Geochem. 38, 198–215.
Clement, A.C., Cane, M.A., Seager, R., 2001. An orbitally driven tropical source for abrupt climate change. J. Clim. 14, 2369–2375.
Collister, J.W., Rieley, G., Stern, B., Eglinton, G., Fry, B., 1994. Compound-specific $\delta^{13}C$ analyses of leaf lipids from plants with differing carbon dioxide metabolisms. Org. Geochem. 21, 619–627.
Coolen, M.J.L., Abbas, B., Van Bleijswijk, J., Hopmans, E.C., Kuypers, M.M.M., Wakeham, S.G., Sinninghe Damsté, J.S., 2007. Putative ammonia-oxidizing Crenarchaeota in suboxic waters of the Black Sea: a basin-wide ecological study using 16S ribosomal and functional genes and membrane lipids. Environ. Microbiol. 9, 1001–1016.
Cranwell, P.A., Eglinton, G., Robinson, N., 1987. Lipids of aquatic organisms as potential contributors to lacustrine sediments. Org. Geochem. 11, 513–527.
Crul, R.C.M., 1995. Limnology and Hydrology of Lake Victoria. UNESCO, Paris, p. 79.
Dahl, K., Broccoli, A., Stouffer, R., 2005. Assessing the role of North Atlantic freshwater forcing in millennial scale climate variability: a tropical Atlantic perspective. Clim. Dyn. 24, 325–346.
Dalfes, H.N., Kukla, G., Weiss, H., 1997. Third Millennium BC Climate Change and Old World Collapse, NATO ASI Series. NATO ASI Series, p. 723.
Dansgaard, W., 1964. Stable isotopes in precipitation. Tellus 16, 436–468.
DeBusk, G.H., 1998. A 37,500-year pollen record from Lake Malawi and implications for the biogeography of afromontane forests. J. Biogeogr. 25, 479–500.
deMenocal, P., Ortiz, J., Guilderson, T., Adkins, J., Sarnthein, M., Baker, L., Yarusinsky, M., 2000. Abrupt onset and termination of the African Humid Period: rapid climate responses to gradual insolation forcing. Quat. Sci. Rev. 19, 347–361.
Diefendorf, A.F., Freeman, K.H., Wing, S.L., Graham, H.V., 2011. Production of n-alkyl lipids in living plants and implications for the geologic past. Geochim. Cosmochim. Acta 75, 7472–7485.
Eglinton, G., Hamilton, R.J., 1967. Leaf epicuticular waxes. Science 156, 1322–1335.
Ehleringer, J.R., Cerling, T.E., Helliker, B.R., 1997. C_4 photosynthesis, atmospheric CO_2, and climate. Oecologia 112, 285–299.
Farrimond, P., Flanagan, R.L., 1996. Lipid stratigraphy of a Flandrian peat bed (Northumberland, UK): comparison with the pollen record. The Holocene 6, 69–74.
Feakins, S.J., Sessions, A.L., 2010. Controls on the D/H ratios of plant leaf waxes in an arid ecosystem. Geochim. Cosmochim. Acta 74, 2128–2141.
Finney, B.P., Scholz, C.A., Johnson, T.C., Trumbore, C., 1996. Late Quaternary lake-level changes of Lake Malawi. In: Johnson, T.C., Odada, E.O. (Eds.), The Limnology, Climatology, and Paleoclimatology of the East African Rift Lakes. Gordon and Breach, Amsterdam, pp. 495–508.
Fish, G.R., 1957. A seiche movement and its effect on the hydrology of Lake Victoria. Colonial Off. Fish. Publ. 10, 1–68.
Fleitmann, D., Burns, S.J., Mangini, A., Mudelsee, M., Kramers, J., Villa, I., Neff, U., Al-Subbary, A.A., Buettner, A., Hippler, D., Matter, A., 2007. Holocene ITCZ and Indian monsoon dynamics recorded in stalagmites from Oman and Yemen (Socotra). Quat. Sci. Rev. 26, 170–188.
Garcin, Y., Schwab, V.F., Gleixner, G., Kahmen, A., Todou, G., Séné, O., Onana, J.-M., Achoundong, G., Sachse, D., 2012. Hydrogen isotope ratios of lacustrine sedimentary n-alkanes as proxies of tropical African hydrology: insights from a calibration transect across Cameroon. Geochim. Cosmochim. Acta 79, 106–126.
Gasse, F., 1977. Evolution of Lake Abhé (Ethiopia and TFAI), from 70,000 B.P. Nature 265, 42–45.
Gasse, F., 2000. Hydrological changes in the African tropics since the Last Glacial Maximum. Quat. Sci. Rev. 19, 189–211.
Gasse, F., Chalié, F., Vincens, A., Williams, M.A.J., Williamson, D., 2008. Climatic patterns in equatorial and southern Africa from 30,000 to 10,000 years ago reconstructed from terrestrial and near-shore proxy data. Quat. Sci. Rev. 27, 2316.
Gasse, F., Ledee, V., Massault, M., Fontes, J.-C., 1989. Water-level fluctuations of Lake Tanganyika in phase with oceanic changes during the last glaciation and deglaciation. Nature 342, 57–59.
Gasse, F., Van Campo, E., 1994. Abrupt post-glacial climate events in West Asia and North Africa monsoon domains. Earth Planet. Sci. Lett. 126, 435–456.
Grice, K., Yu, H., Zhou, Y.P., Stuart-Williams, H., Farquhar, G.D., 2008. Biosynthetic and environmental effects on the stable carbon isotopic compositions of anteiso-(3-methyl) and iso-(2-methyl) alkanes in tobacco leaves. Phytochemistry 69, 2807–2814.
Hastenrath, S., Kutzbach, J.E., 1983. Paleoclimatic estimates from water and energy budgets of East African Lakes. Quat. Res. 19, 141–153.
Hastenrath, S., Nicklis, A., Greischar, L., 1993. Atmospheric-hydrospheric mechanisms of climate anomalies in the western equatorial Indian Ocean. J. Geophys. Res. 98, 20219–20235.
Hatch, M.D., 1987. C_4 photosynthesis: a unique blend of modified biochemistry, anatomy and ultrastructure. Biochim. Biophys. Acta 895, 81–106.
Hopmans, E.C., Weijers, J.W.H., Schefuß, E., Herfort, L., Sinninghe Damsté, J.S., 2004. A novel proxy for terrestrial organic matter in sediments based on branched and isoprenoid tetraether lipids. Earth Planet. Sci. Lett. 224, 107–116.
Hou, J., D'Andrea, W.J., Huang, Y., 2008. Can sedimentary leaf waxes record D/H ratios of continental precipitation? Field, model, and experimental assessments. Geochim. Cosmochim. Acta 72, 3503–3517.
Hou, J., D'Andrea, W.J., MacDonald, D., Huang, Y., 2007. Evidence for water use efficiency as an important factor in determining the δD values of tree leaf waxes. Org. Geochem. 38, 1251–1255.
Huang, Y., Dupont, L., Sarnthein, M., Hayes, J.M., Eglinton, G., 2000. Mapping of C_4 plant input from North West Africa into North East Atlantic sediments. Geochim. Cosmochim. Acta 64, 3505–3513.
Indermuhle, A., Stocker, T.F., Joos, F., Fischer, H., Smith, H.J., Wahlen, M., Deck, B., Mastroianni, D., Tschumi, J., Blunier, T., Meyer, R., Stauffer, B., 1999. Holocene carbon-cycle dynamics based on CO_2 trapped in ice at Taylor Dome, Antarctica. Nature 398, 121–126.
Johnson, T.C., Brown, E.T., McManus, J., Barry, S., Barker, P.A., Gasse, F., 2002. A high-resolution paleoclimate record spanning the past 25,000 years in southern east Africa. Science 296, 113–132.
Johnson, T.C., Kelts, K., Odada, E., 2000. The Holocene history of Lake Victoria. Ambio 29, 2–11.
Johnson, T.C., Scholz, C.A., Talbot, M.R., Kelts, K., Ricketts, R.D., Ngobi, G., Beuning, K., Ssemmanda, I., McGill, J.W., 1996. Late Pleistocene desiccation of Lake Victoria and rapid evolution of cichlid fishes. Science 273, 1091–1093.
Jolly, D., Harrison, S.P., Damnati, B., Bonnefille, R., 1998. Simulated climate and biomes of Africa during the late quaternary: comparison with pollen and lake status data. Quat. Sci. Rev. 17, 629–657.
Kahmen, A., Dawson, T.E., Vieth, A., Sachse, D., 2011. Leaf wax n-alkane dD values are determined early in the ontogeny of Populus trichocarpa leaves when grown under controlled environmental conditions. Plant Cell. Environ. 34, 1639–1651.
Kalnay, E., Kanamitsu, M., Kistler, R., Collins, W., Deaven, D., Gandin, L., Iredell, M., Saha, S., White, G., Woollen, J., Zhu, Y., Leetmaa, A., Reynolds, R., Chelliah, M., Ebisuzaki, W., Higgins, W., Janowiak, J., Mo, K.C., Ropelewski, C., Wang, J., Jenne, R., Joseph, D., 1996. The NCEP/NCAR 40-Year reanalysis project. Bull. Am. Meteorol. Soc. 77, 437–471.
Kendall, R.L., 1969. An ecological history of the Lake Victoria basin. Ecol. Monogr. 39, 121–176.
Kim, J.-H., van der Meer, J., Schouten, S., Helmke, P., Willmott, V., Sangiorgi, F., Koç, N., Hopmans, E.C., Sinninghe Damsté, J.S., 2010. New indices and calibrations derived from the distribution of crenarchaeal isoprenoid tetraether lipids: implications for past sea surface temperature reconstructions. Geochim. Cosmochim. Acta 74, 4639–4654.
Konecky, B.L., Russell, J.M., Johnson, T.C., Brown, E.T., Berke, M.A., Werne, J.P., Huang, Y., 2011. Atmospheric circulation patterns during late Pleistocene climate changes at Lake Malawi, Africa. Earth Planet. Sci. Lett. 312, 318–326.
Konneke, M., Bernhard, A.E., de la Torre, J.R., Walker, C.B., Waterbury, J.B., Stahl, D.A., 2005. Isolation of an autotrophic ammonia-oxidizing marine archaeon. Nature 437, 543–546.

Krishnan, R., Swapna, P., 2009. Significant influence of the boreal summer monsoon flow on the Indian Ocean response during dipole events. J. Clim. 22, 5611–5634.
Leroux, M., 2001. Meteorology and Climate of Tropical Africa. Springer-Praxis, London.
Levin, N.E., Zipser, E.J., Cerling, T.E., 2009. Isotopic composition of waters from Ethiopia and Kenya: insights into moisture sources for eastern Africa. J. Geophys. Res. 114, D23306.
Li, C., Sessions, A.L., Valentine, D.L., Thiagarajan, N., 2011. D/H variation in terrestrial lipids from Santa Barbara Basin over the past 1400 years: a preliminary assessment of paleoclimatic relevance. Org. Geochem. 42, 15–24.
Lisiecki, L.E., Raymo, M.E., 2005. A Pliocene-Pleistocene stack of 57 globally distributed benthic $\delta^{18}O$ records. Paleoceanography 20, PA1003.
Liu, Z., Henderson, A.C.G., Huang, Y., 2008. Regional moisture source changes inferred from Late Holocene stable isotope records. Ad. Atmos. Sci. 25, 1021–1028.
Liu, Z., Otto-Bliesner, B., Kutzbach, J., Li, L., Shields, C., 2003. Coupled climate simulation of the evolution of global monsoons in the Holocene. J. Clim. 16, 2472–2490.
Livingstone, D.A., Clayton, W.D., 1980. An altitudinal cline in tropical African grass floras and its paleoecological significance. Quat. Res. 13, 392–402.
Magny, M., Vannière, B., Zanchetta, G., Fouache, E., Touchais, G., Petrika, L., Coussot, C., Walter-Simonnet, A.-V., Arnaud, F., 2009. Possible complexity of the climatic event around 4300—3800 cal. BP in the central and western Mediterranean. The Holocene 19, 823–833.
Majoube, M., 1971. Fractionment en oxygene-18 et en deuterium entré l'eau at sa vapeur Jour. Chem. Phys. 10, 1423–1436.
Makou, M.C., Hughen, K.A., Xu, L., Sylva, S.P., Eglinton, T.I., 2007. Isotopic records of tropical vegetation and climate change from terrestrial vascular plant biomarkers preserved in Cariaco Basin sediments. Org. Geochem. 38, 1680–1691.
Mohtadi, M., Lückge, A., Steinke, S., Groeneveld, J., Hebbeln, D., Westphal, N., 2010. Late Pleistocene surface and thermocline conditions of the eastern tropical Indian Ocean. Quat. Sci. Rev. 29, 887–896.
Mortazavi, B., Conte, M.H., Chanton, J.P., Smith, M.C., Weber, J.C., Crumsey, J., Ghashghaie, J., 2009. Does the ^{13}C of foliage-respired CO_2 and biochemical pools reflect the ^{13}C of recently assimilated carbon? Plant Cell. Environ. 32, 1310–1323.
Nicholson, S.E., 1988. Historical fluctuations of Lake Victoria and other lakes in the Northern Rift Valley of East Africa. In: Lehman, S.J. (Ed.), Environmental Change and Response in East African Lakes. Kluwer Academic Publishers, Amsterdam, pp. 7–35.
Nicholson, S.E., 1996. A review of climate dynamics and climate variability in eastern Africa. In: Johnson, T.C., Odada, E.O. (Eds.), The Limnology, Climatology, and Paleoclimatology of the East African Rift Lakes. Gordon and Breach, Amsterdam, pp. 25–56.
Nicholson, S.E., Selato, J.C., 2000. The influence of La Niña on African rainfall. Int. J. Clim. 20, 1761–1776.
Niedermeyer, E.M., Schefuß, E., Sessions, A.L., Mulitza, S., Mollenhauer, G., Schulz, M., Wefer, G., 2010. Orbital- and millennial-scale changes in the hydrologic cycle and vegetation in the western African Sahel: insights from individual plant wax δD and $\delta^{13}C$. Quat. Sci. Rev. 29, 2996–3005.
O'Leary, M.H., 1981. Carbon isotope fractionation in plants. Phytochemistry 20, 553–567.
Polissar, P.J., Freeman, K.H., 2010. Effects of aridity and vegetation on plant-wax δD in modern lake sediments. Geochim. Cosmochim. Acta 74, 5785–5797.
Powers, L.A., Johnson, T.C., Werne, J.P., Castañeda, I., Hopmans, E.C., Sinninghe Damsté, J.S., Schouten, S., 2005. Large temperature variability in the southern African tropics since the Last Glacial Maximum. Geophys. Res. Lett. 32, L08706. http://dx.doi.org/10.1029/2004GL022014.
Powers, L.A., Werne, J.P., Van der woude, A.J., Sinninghe Damsté, J.S., Hopmans, E.C., Schouten, S., 2010. Applicability and calibration of the TEX_{86} paleothermometer in lakes. Org. Geochem. 41, 404–413.
Prentice, I.C., Webb, T., 1986. Pollen percentages, tree abundances and the Fagerlind effect. J. Quat. Sci. 1, 35–43.
Rieley, G., Collister, J.W., Stern, B., Eglinton, G., 1993. Gas chromatography/isotope ratio mass spectrometry of leaf wax *n*-alkanes from plants of differing carbon dioxide metabolisms. Rapid Commun. Mass. Spectrom. 7, 488–491.
Rommerskirchen, F., Eglinton, G., Dupont, L., Güntner, U., Wenzel, C., Rullkötter, J., 2003. A north to south transect of Holocene southeast Atlantic continental margin sediments: relationship between aerosol transport and compound-specific $\delta^{13}C$ land plant biomarker and pollen records. Geochem. Geophys. Geosyst. 4, 1101.
Rommerskirchen, F., Plader, A., Eglinton, G., Chikaraishi, Y., Rullkötter, J., 2006. Chemotaxonomic significance of distribution and stable carbon isotopic composition of long-chain alkanes and alkan-1-ols in C4 grass waxes. Org. Geochem. 37, 1303–1332.
Rozanski, K., Araguas-Araguas, L., Gonfiantini, 1996. Isotope patterns of precipitation in the East African region. In: Johnson, T.C., Odada, E. (Eds.), Limnology, Climatology and Paleoclimatology of the East African Lakes. Gordon and Breach Publishers, Amsterdam.
Rozanski, K., Araguas-Araguas, L., Gonfiantini, R., 1993. Isotopic patterns in modem global precipitation. In: Swart, P.K., Lohmann, K.C., McKenzie, J.A., Savin, S. (Eds.), Climate Change in Continental Isotopic Records. AGU Monograph, pp. 1–36.
Russell, J., Talbot, M.R., Haskell, B.J., 2003. Mid-Holocene climate change in Lake Bosumtwi, Ghana. Quat. Res. 60, 133–141.
Sachse, D., Billault, I., Bowen, G.J., Chikaraishi, Y., Dawson, T.E., Feakins, S.J., Freeman, K.H., Magill, C.R., McInerney, F.A., van der Meer, M.T.J., Polissar, P., Robins, R.J., Sachs, J.P., Schmidt, H.-L., Sessions, A.L., White, J.W.C., West, J.B., Kahmen, A., 2012. Molecular paleohydrology: interpreting the hydrogen-isotopic composition of lipid biomarkers from photosynthesizing organisms. Annu. Rev. Earth Planet. Sci. 40, 221–249.
Sachse, D., Gleixner, G., Wilkes, H., Kahmen, A., 2010. Leaf wax *n*-alkane δD values of field-grown barley reflect leaf water δD values at the time of leaf formation. Geochim. Cosmochim. Acta 74, 6741–6750.
Sachse, D., Radke, J., Gleixner, G., 2004. Hydrogen isotope ratios of recent lacustrine sedimentary *n*-alkanes record modern climate variability. Geochim. Cosmochim. Acta 68, 4877–4889.
Saji, N.H., Goswami, B.N., Vinayachandran, P.N., Yamagata, T., 1999. A dipole mode in the tropical Indian Ocean. Nature 401, 360–363.
Schefuß, E., Kuhlmann, H., Mollenhauer, G., Prange, M., Patzold, J., 2011. Forcing of wet phases in southeast Africa over the past 17,000 years. Nature 480, 509–512.
Schefuß, E., Schouten, S., Jansen, J.H.F., Sinninghe Damsté, J.S., 2003. African vegetation controlled by tropical sea surface temperatures in the mid-Pleistocene period. Nature 422, 418–421.
Schefuß, E., Schouten, S., Schneider, R.R., Sinninghe Damsté, J.S., 2005. Central African hydrologic changes during the past 20,000 years. Nature 437, 1003–1006.
Schouten, S., Hopmans, E.C., Schefuß, E., Sinninghe Damsté, J.S., 2002. Distributional variations in marine crenarchaeotal membrane lipids: a new tool for reconstructing ancient sea water temperatures? Earth Planet. Sci. Lett. 204, 265–274.
Schouten, S., Huguet, C., Hopmans, E.C., Kienhuis, M.V.M., Sinninghe Damsté, J.S., 2007. Analytical methodology for TEX_{86} paleothermometry by high-performance liquid chromatography/atmospheric pressure chemical ionization-mass spectrometry. Anal. Chem. 79, 2940–2944.
Schrag, D.P., Hampt, G., Murray, D.W., 1996. Pore fluid constraints on the temperature and oxygen isotopic composition of the glacial ocean. Science 272, 1930–1932.
Sene, K.J., Plinston, D.T., 1994. A review and update of the hydrology of Lake Victoria in East Africa. Hydro. Sci. J. 39, 47–63.
Sinninghe Damsté, J.S., Verschuren, D., Ossebaar, J., Blokker, J., van Houten, R., van der Meer, M.T.J., Plessen, B., Schouten, S., 2011. A 25,000-year record of climate-induced changes in lowland vegetation of eastern equatorial Africa revealed by the stable carbon-isotopic composition of fossil plant leaf waxes. Earth Planet. Sci. Lett. 302, 236–246.
Smith, F.A., Freeman, K.H., 2006. Influence of physiology and climate on δD of leaf wax *n*-alkanes from C_3 and C_4 grasses. Geochim. Cosmochim. Acta 70, 1172–1187.
Stager, J.C., Cumming, B.F., Meeker, L.D., 2003. A 10,200 year high-resolution diatom record from Pilkington Bay, Lake Victoria, Uganda. Quat. Res. 59, 172–181.
Stager, J.C., Mayewski, P.A., 1997. Abrupt early to mid-Holocene climatic transition registered at the equator and the poles. Science 276, 1834–1836.
Still, C.J., Powell, R.L., 2010. Continental-scale distributions of vegetation stable carbon isotope ratios. In: West, J.B., Bowen, G.J., Dawson, T.E., Tu, K.P. (Eds.), Isoscapes. Springer, Netherlands, pp. 179–193.
Taiz, L., Zeiger, E., 1998. Plant Physiology, second ed. Sinauer Assoc., Sunderland, MA.
Talbot, M.R., Filippi, M.L., Jensen, N.B., Tiercelin, J.-J., 2007. An abrupt change in the African monsoon at the end of the Younger Dryas. Geochem. Geophys. Geosyst. 8, Q03005.
Talbot, M.R., Lærdal, T., 2000. The Late Pleistocene – Holocene palaeolimnology of Lake Victoria, East Africa, based upon elemental and isotopic analyses of sedimentary organic matter. J. Paleolimnol. 23, 141–164.
Talbot, M.R., Livingstone, D.A., Palmer, P., Maley, J., Melack, J.M., Delibrias, G., Gulliksen, S., 1984. Preliminary results from sediment cores from Lake Bosumtwi, Ghana. Palaeoecol. Afr. 16, 173–192.
Talling, J.F., 1957. Some observations on the stratification of Lake Victoria. Limnol. Oceanogr. 2, 213–221.
Thompson, L.G., Mosley-Thompson, E., Davis, M.E., Henderson, K.A., Brecher, H.H., Zagorodnov, V.S., Mashiotta, T.A., Lin, P.-N., Mikhalenko, V.N., Hardy, D.R., Beer, J., 2002. Kilimanjaro ice core records: evidence of Holocene climate change in tropical Africa. Science 298, 589–593.
Tierney, J.E., Russell, J.M., Huang, Y., Sinninghe Damsté, J.S., Hopmans, E.C., Cohen, A.S., 2008. Northern Hemisphere controls on tropical southeast African climate during the past 60,000 years. Science 322, 252–255.
Tierney, J.E., Russell, J.M., Huang, Y.S., 2010. A molecular perspective on Late Quaternary climate and vegetation change in the Lake Tanganyika basin, East Africa. Quat. Sci. Rev. 29, 787–800.
Tierney, J.E., Russell, J.M., Sinninghe Damsté, J.S., Huang, Y., Verschuren, D., 2011. Late quaternary behavior of the East African monsoon and the importance of the Congo Air Boundary. Quat. Sci. Rev. 30, 798–807.
Timmermann, A., An, S.I., Krebs, U., Goosse, H., 2005. ENSO suppression due to weakening of the North Atlantic thermohaline circulation. J. Clim. 18, 3122–3139.
Timmermann, A., Okumura, Y., An, S.I., Clement, A., Dong, B., Guilyardi, E., Hu, A., Jungclaus, J.H., Renold, M., Stocker, T.F., Stouffer, R.J., Sutton, R., Xie, S.P., Yin, J., 2007. The influence of a weakening of the Atlantic Meridional Overturning Circulation on ENSO. J. Clim. 20, 4899–4919.
Tipple, B.J., Pagani, M., 2007. The early origins of terrestrial C_4 photosynthesis. Annu. Rev. Earth Planet. Sci. 35, 435–461.
Tjallingii, R., Claussen, M., Stuut, J.B.W., Fohlmeister, J., Jahn, A., Bickert, T., Lamy, F., Röhl, U., 2008. Coherent high- and low-latitude control of the northwest African hydrological balance. Nat. Geosci. 1, 670–675.

Verschuren, D., Sinninghe Damste, J.S., Moernaut, J., Kristen, I., Blaauw, M., Fagot, M., Haug, G.H., 2009. Half-precessional dynamics of monsoon rainfall near the East African Equator. Nature 462, 637–641.

Vincens, A., Buchet, G., Servant, M., collaborators, E., 2010. Vegetation response to the "African Humid Period" in central Cameroon (7°N) – new pollen insight from Lake Mbalang. Clim. Past 6, 281–294.

Vogts, A., Moossen, H., Rommerskirchen, F., Rullkötter, J., 2009. Distribution patterns and stable carbon isotopic composition of alkanes and alkan-1-ols from plant waxes of African rain forest and savanna C3 species. Org. Geochem. 40, 1037–1054.

Wakeham, S.G., Pease, T.K., 1992. Lipid Analysis in Marine Particles and Sediment Samples. Skidaway Institute of Oceanography, Savannah, GA.

Wang, Y., Cheng, H., Edwards, R.L., Kong, X., Shao, X., Chen, S., Wu, J., Jiang, X., Wang, X., An, Z., 2008. Millennial- and orbital-scale changes in the East Asian monsoon over the past 224,000 years. Nature 451, 1090–1093.

Weijers, J.W.H., Schefuß, E., Schouten, S., Sinninghe Damsté, J.S., 2007. Coupled thermal and hydrological evolution of tropical Africa over the last deglaciation. Science 315, 1701–1704.

Weijers, J.W.H., Schouten, S., Spaargaren, O.C., Damste, J.S.S., 2006. Occurrence and distribution of tetraether membrane lipids in soils: implications for the use of the TEX_{86} proxy and the BIT index. Org. Geochem. 37, 1680–1693.

Weninger, B., Jöris, O., Danzeglocke, U., 2011. CalPal-2007. http://www.calpal-online.de/.

White, F., 1983. Vegetation of Africa – a Descriptive Memoir to Accompany the Unesco/AETFAT/UNSO Vegetation Map of Africa, Paris.

Wuchter, C., Abbas, B., Coolen, M.J.L., Herfort, L., van Bleijswijk, J., Timmers, P., Strous, M., Teira, E., Herndl, G.J., Middelburg, J.J., Schouten, S., Sinninghe Damsté, J.S., 2006. Archaeal nitrification in the ocean. PNAS 103, 12317–12322.

Wuchter, C., Schouten, S., Coolen, M.J.L., Sinninghe Damsté, J.S., 2004. Temperature-dependent variation in the distribution of tetraether membrane lipids of marine Crenarchaeota: implications for TEX_{86}. Paleotherm. Paleoceanogr 19. http://dx.doi.org/10.1029/2004PA001041.

Yang, H., Huang, Y., 2003. Preservation of lipid hydrogen isotope ratios in Miocene lacustrine sediments and plant fossils at Clarkia, northern Idaho, USA. Org. Geochem. 34, 413.

Yin, X., Nicholson, S.E., 1998. The water balance of Lake Victoria. Hydro. Sci. 43, 789–811.

Zhang, X., Gillespie, A.L., Sessions, A.L., 2009. Large D/H variations in bacterial lipids reflect central metabolic pathways. PNAS 106, 12580–12586.

Zhou, Y., Grice, K., Chikaraishi, Y., Stuart-Williams, H., Farquhar, G.D., Ohkouchi, N., 2011. Temperature effect on leaf water deuterium enrichment and isotopic fractionation during leaf lipid biosynthesis: results from controlled growth of C_3 and C_4 land plants. Phytochemistry 72, 207–213.